

CLAN: A Contrastive Learning based Novelty Detection Framework for Human Activity Recognition

HYUNJU KIM, Korea Advanced Institute of Science & Technology, South Korea

DONGMAN LEE, Korea Advanced Institute of Science & Technology, South Korea

In ambient assisted living, human activity recognition from time series sensor data mainly focuses on predefined activities, often overlooking new activity patterns. We propose *CLAN*, a two-tower contrastive learning-based novelty detection framework with diverse types of negative pairs for human activity recognition. It is tailored to challenges with human activity characteristics, including the significance of temporal and frequency features, complex activity dynamics, shared features across activities, and sensor modality variations. The framework aims to construct invariant representations of known activity robust to the challenges. To generate suitable negative pairs, it selects data augmentation methods according to the temporal and frequency characteristics of each dataset. It derives the key representations against meaningless dynamics by contrastive and classification losses-based representation learning and score function-based novelty detection that accommodate dynamic numbers of the different types of augmented samples. The proposed two-tower model extracts the representations in terms of time and frequency, mutually enhancing expressiveness for distinguishing between new and known activities, even when they share common features. Experiments on four real-world human activity datasets show that CLAN surpasses the best performance of existing novelty detection methods, improving by 8.3%, 13.7%, and 53.3% in AUROC, balanced accuracy, and FPR@TPR0.95 metrics respectively.

CCS Concepts: • **Human-centered computing** → **Ubiquitous and mobile computing design and evaluation methods**.

Additional Key Words and Phrases: novelty detection, human activity recognition, contrastive learning, time series sensor data

ACM Reference Format:

Hyunju Kim and Dongman Lee. 2024. CLAN: A Contrastive Learning based Novelty Detection Framework for Human Activity Recognition. 0, 0 (January 2024), 41 pages. <https://doi.org/XXXXXXXX.XXXXXXX>

1 INTRODUCTION

The extensive adoption of Internet of Things (IoT) technologies has paved the way for users to streamline their lives and enhance their productivity through the utilization of intelligent applications such as customized services, healthcare systems, and surveillance systems [42, 51, 61, 88]. Such applications generate time-series sensor data according to a user's behavior. Human activity recognition (HAR) [9, 41, 77], which extracts the user's activity patterns automatically based on the data, has become a pivotal technology supporting the functioning of an ambient assisted living (AAL) environment [18, 52]. Researchers have recently leveraged deep learning models to HAR, ranging from Recurrent Neural Networks (RNNs) and Generative Adversarial Networks (GANs) to Transformers, or hybrids of them [14, 16, 26, 44, 47, 49, 54, 58, 87]. These models automatically extract important features from the user behavioral data, significantly improving the accuracy and efficiency of the HAR.

Authors' addresses: Hyunju Kim, Korea Advanced Institute of Science & Technology, Daejeon, South Korea, iplay93@kaist.ac.kr; Dongman Lee, Korea Advanced Institute of Science & Technology, Daejeon, South Korea, dlee@kaist.ac.kr.

Permission to make digital or hard copies of all or part of this work for personal or classroom use is granted without fee provided that copies are not made or distributed for profit or commercial advantage and that copies bear this notice and the full citation on the first page. Copyrights for components of this work owned by others than ACM must be honored. Abstracting with credit is permitted. To copy otherwise, or republish, to post on servers or to redistribute to lists, requires prior specific permission and/or a fee. Request permissions from permissions@acm.org.

© 2024 Association for Computing Machinery.

XXXX-XXXX/2024/1-ART \$15.00

<https://doi.org/XXXXXXXX.XXXXXXX>

The previous approaches primarily concentrate on predefined activities. However, it is equally crucial to uncover patterns in new activities as they complement and strengthen each other [27]. The American Time Use Survey, conducted by the U.S. Bureau of Labor Statistics [1, 17], reveals a variety of over 462 distinct activities engaged in by individuals in their daily lives, which can further vary depending on environmental factors and individual preferences. Given the intricate and diverse nature of human activities [13], it is unfeasible to exhaustively define every conceivable activity in the real world, leaving room for the emergence of new activities. Therefore, it is essential for HAR systems to be capable of detecting and adapting to these new activities in order to be applicable in dynamic and evolving real-world environments.

Detecting a new activity is equivalent to identifying novel patterns from a new class that do not exist in the training data distribution, which is commonly known as novelty detection [2, 57, 66, 82]. Existing novelty detection methods for HAR have mainly focused on detecting novelty in individual data points or subsequences within an activity that deviates from repetition patterns such as routines, trends, or seasonality [20, 48, 78, 81]. However, in real-world environments involving interactions with various objects and other users and temporal dynamics inherent in user behavior [3, 28], the aforementioned methods face difficulty in detecting novelty in user activity. That is, finding constant patterns from repetitions of individual data points or subsequences is not enough to discern a new activity. There needs a new mechanism to detect novelty with invariant representations for a known activity at the instance level.

Computing vision has developed many cutting-edge learning techniques for detecting novelty at the instance level. They develop various methods for novelty detection, including density-based [25, 83], distance-based [8, 68, 74], reconstruction-based [12, 40, 59, 65], and classification-based [30, 63, 67, 73] approaches. Recent research [8, 12, 15, 73] using contrastive learning has shown a strong ability to learn invariant representations for detecting novel patterns with instance discrimination [80]. This self-supervised approach involves grouping similar views (positives) while simultaneously pushing apart dissimilar views (negatives), for each instance. Recent advances in contrastive learning studies [12, 73] find that forcing samples that are strongly shifted from the original sample as negatives helps in the improvement of novelty detection performance.

The existing contrastive learning methods for computer vision show potential in deriving invariant representations for detecting novel patterns. However, they do not fit well with HAR which exploits time series sensor data. This results in new challenges as follows:

- The existing studies are designed to extract spatial or color features from visual data, making them unsuitable for capturing complex temporal correlations or sensor frequencies inherent in the time series sensor data [50, 71, 85, 86]. Furthermore, these properties are varied according to the sensor modality of each dataset. It is challenging to apply the prior knowledge of data augmentation [15, 53] for generating positives or negatives depending on image features, such as de-colorization or rotation, to the time series sensor data. In addition, their encoders extract representations for spatial information using only convolutional layers such as ResNet [34], which does not effectively capture long-range temporal dependencies or frequency patterns.
- It is assumed in computer vision that data is well-structured and clean. On the other hand, time series sensor data exhibits temporal dynamics even in the same activity due to factors such as inherent dynamics of user behavior, the presence of noise, missing values, or irregular sampling intervals [3, 50]. If only a single type of data augmentation is applied for generating samples to push away, time series data is trained to counter one aspect of variation (e.g. timing) and be insensitive to other types of variation (e.g. scale). This singular focus on one aspect leads to the extraction of biased representations, and unimportant patterns from other types of variations are unintentionally incorporated into invariant representations. In essence, this reduces the overall generality and robustness of activity representations.

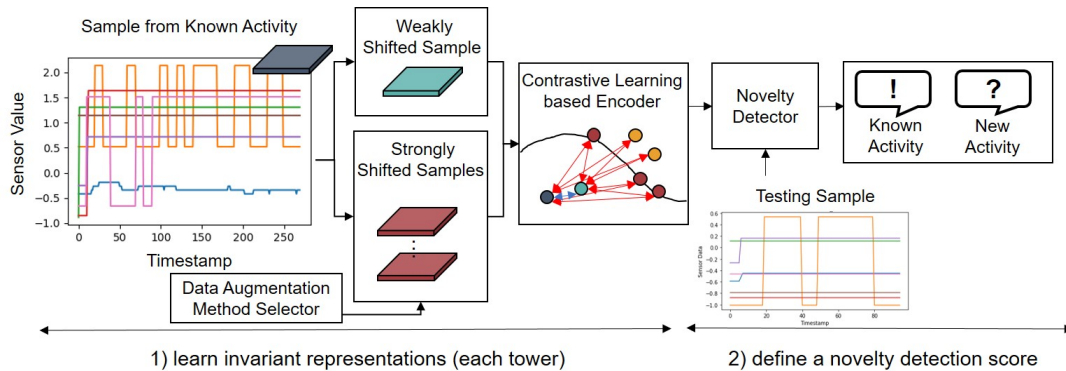


Fig. 1. An illustrative example of how CLAN works in time series sensor data related to human activities. Similar to common novelty detection mechanisms, it is divided into two phases: 1) learning invariant representations for a known class and 2) defining a novelty detection score.

- The previous studies detect novel patterns like color, shape, and texture for a new class extracted from numerous pixels [29]. However, there exist inherent limitations in time series sensor data driven by a human activity to express the representative properties of each activity due to a relatively small amount of sensor types and associated values. This makes it difficult to create clear distinctiveness between activities. For example, activities such as *Small talk* (known activity) and *Technical meeting* (new activity) can share a similar temporal subsequence of sound or light sensors, which cause some samples in *Technical meeting* to be misclassified as *Small talk*, that is, known activity due to blurred representation boundaries between the two activities in the time domain.

In this paper, we propose CLAN, Two Tower Contrastive Learning with Diverse Data Augmentation based Novelty Detection Framework, for effectively detecting new activities in time series sensor data. To the best of our knowledge, it is the first time to detect novelties using contrastive learning in ambient assistant living (AAL) environments. Figure 1 describes an example scenario for how CLAN detects the key representations of a new activity. The data augmentation method selector of CLAN supports determining data augmentation techniques that produce strongly shifted samples by considering temporal or frequency properties in the time series data. Although it's challenging to visually gauge the degree of data shift post-augmentation, as depicted in Figure 2, CLAN automatically chooses augmentation methods based on the classification performance of original versus augmented samples. And, the encoder learns key representations of the known activity against meaningless temporal dynamics by comparing diverse types of the augmented samples to the original samples. To facilitate this comparison, we design a contrastive loss function that adapts the number of instances to be pushed apart based on the number of augmented samples. To lead to more distinctive and informative features for distinguishing new activity from known activity, even when they have common features, CLAN employs a two-tower model. This identifies different facets of the time series sensor data within the time and frequency domains, creating two distinct representations for each single sample. Subsequently, the novelty detector of CLAN identifies new activity samples by holistically determining similarity and classifying likelihood metrics based on the acquired representations for each facet. The main contributions of our approach are summarized as follows:

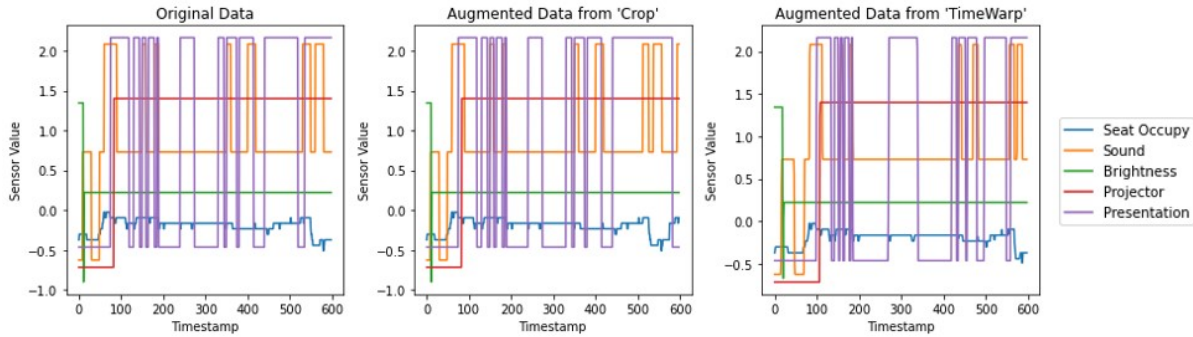


Fig. 2. Visualization of augmented data after applying *Crop* and *TimeWarp* to a sample in activity *Seminar*. The left figure represents the data sequence of the original sample, the middle figure represents the data sequence after applying the *Crop* method, and the right figure represents the data sequence after applying the *TimeWarp* method. These demonstrate that it is difficult for a human observer to gauge the degree of shift that occurred in the augmented data.

- We propose a two-tower self-supervised-based new activity detection framework for sensor-based time series, CLAN, which constructs invariant representations using contrastive learning that simultaneously compares multiple types of negatives in the time and frequency domains, respectively.
- We devise a classification-based selector that automatically decides data augmentation methods for generating powerful positives and negatives according to property of each time series sensor dataset.
- We evaluate the novelty detection performance of the CLAN by comparing the seven representative novelty detection approaches on four real human activity datasets, including DOO-RE [43], CASAS [70], Opportunity [62] and ARAS [5]. Through both quantitative and qualitative evaluations, we demonstrate that CLAN derives high-quality representations for distinguishing between known and new activity. All experiments are performed in unsupervised settings without activity labels, implying that CLAN potentially responds to data labeling or data size problems that may arise from time series sensor data.

This paper is organized as follows. In Section 2, we present the existing studies of HAR and novelty detection methods. We define a problem statement in Section 3 and provide an overview of CLAN in Section 4, including its internal detailed modules and learning mechanisms. Section 5 analyzes the effectiveness of CLAN in novelty detection. Finally, we conclude the paper and discuss future work in Section 6.

2 RELATED WORK

In this section, we elucidate the research that we draw inspiration from while developing CLAN and discuss their constraints in detecting novel patterns in time series sensor data.

2.1 Human Activity Recognition using Time Series Sensor Data

Human Activity Recognition (HAR) with ambient sensors has become an important fundamental technology for providing optimal user services with minimal user disruption [18, 52]. The related HAR studies utilize various types of ambient sensors, such as user-driven sensors (e.g. motion sensor), environment-driven sensors (e.g. temperature sensor), or object-driven sensors (e.g. light status sensor) [9, 41]. Recent advancements in this area have led to methods that either utilize or hybridize different deep learning techniques [13, 26, 77], facilitating more comprehensive and sophisticated modeling of human activity data. In recent times, incorporating the Transformer’s multi-head attention mechanism into HAR has demonstrated impressive results by effectively capturing temporal dependencies. As a result, many current research endeavors [26, 44, 45, 47, 49, 79, 84] explore

Transformer variants or self-attention mechanisms for HAR. A series of recent studies [21, 71, 85, 86] have discovered that sensor frequency information is important for representing time series data beyond just finding temporal dependencies patterns. Analyzing the time domain allows us to understand statistical characteristics like the average and variation of individual sensors' values, as well as the temporal correlations between different sensors. Meanwhile, exploring the frequency domain offers insights into how frequently each sensor activates and the overall pattern of sensor occurrences within each activity. These time and frequency domains are inherent in all sensor-driven time series data [50], and leveraging both domains is crucial for a comprehensive analysis of any datasets related to human activities. The previous approaches for HAR have demonstrated notable success, however, they fall short in their ability to adapt and remain flexible when faced with new activities that may emerge in dynamic and evolving real-world environments [1, 13, 17].

2.2 Novelty Detection

Novelty detection, used in various applications, is the task of detecting unique or new patterns within data that fall outside the confines of the training data distribution [57, 66, 82]. In sensor-based time series analysis, novelty detection methodologies traditionally center their efforts on singling out novelties at the granularity of individual data points or subsequences [20, 48, 81] levels, especially in scenarios involving datasets with repeating patterns. The complexity of human activity, with its intricate temporal dynamics [3], makes it challenging to spot new patterns at these levels. In computer vision and natural language processing [46, 66, 82], cutting-edge studies have yielded a diverse range of sophisticated techniques tailored for detecting novelty at the instance level. These novelty detection methods are broadly categorized into four types [82]: density-based [25, 83], distance-based [8, 68, 74], reconstruction-based [12, 40, 59, 65], and classification-based [30, 63, 67, 73]. The latter two are particularly prominent, offering effective results in various applications. The common mechanism that the antecedent approaches share is 1) leveraging encoding and model learning techniques that enable the extraction of invariant representations for a known class, and then 2) estimating novelty detection scores that serve as differentiation criteria between known and new classes (See Figure 1). Reconstruction-based techniques commonly employ encoder-decoder frameworks that are trained with in-distribution data, utilizing models like autoencoders (AEs) [7, 65] or Generative Adversarial Networks (GANs) [31, 59]. One example is OCGAN, introduced by Perera *et al.* [68], which uses a denoising auto-encoder network for one-class novelty detection. This approach constrains the latent space to exclusively represent the given known class by employing bounded support, adversarial training in the latent space, and gradient-descent-based sampling. Classification-based approaches leverage the output of a neural network classifier as a novelty detection score to evaluate whether incoming data is an instance of the new class or not. Ruff *et al.* [63] develop a kernel-based one-class classification approach called DeepSVDD, which trains deep neural networks with a minimum volume estimation objective that creates a compact and representative hypersphere boundary for a known class. Recently, self-supervised based research [10, 12, 73] with contrastive learning has demonstrated advanced abilities to detect novel patterns.

2.3 Contrastive Learning

Contrastive learning [15, 80] commonly extracts invariant representations by maximizing the similarity between the representations of positive pairs and minimizing the similarity between the negative pairs. The methods for applying contrastive learning to time series sensor data [16, 22, 24, 38, 86] continue to be proposed these days, however, they mainly focus on how to recognize predefined activities and only leverage positive pairs. Contrastive learning [8, 10, 15, 39, 73] in computer vision is used to detect new class instances by training a model to extract invariant representations of known classes and detecting new patterns that are not associated with them. The important point to note here is that novelty detection technologies find it difficult to acquire information about new classes during training, therefore, methods are being devised to obtain better representations using

augmented samples. For example, Tack *et al.* [73] introduce the CSI framework, which aims to obtain invariant representations of inliers by using strongest shifted samples (e.g. Rotation) as negatives in contrastive learning. Despite its promise, the existing techniques are difficult to effectively capture the significant features related to the temporal or frequency properties of time series sensor data and use them for novelty detection. In this paper, we build an effective novelty detection framework designed for sensor-based time series data using contrastive learning for the first time.

3 PRELIMINARIES

In this section, we define notation terms and use them to define a problem statement for detecting a new human activity.

3.1 Definition 1. Time Series Sensor Data and Distribution

For a given training dataset $\mathcal{X} = \{x_i \mid i = 1, \dots, N\}$, each sensor-based time series sample $x_i \in \mathbb{R}^{D \times L}$ is composed of states acquired from D sensors over a duration of L timestamps, where $D = 1$ if the dataset is univariate and $D > 1$ if it is multivariate. N denotes the number of samples. In the AAL domain, one sample refers to one activity episode consisting of a series of human action sequences [18, 52]. For simplicity of terminology, if a specific sample is not indicated, the sample is written as x . The distribution of \mathcal{X} is denoted by $p(x)$, meaning in-distribution, and a sample of $p(x)$ is recognized as one of the known activities.

3.2 Definition 2. Time and Frequency Domain of Each Sample

Each sample x is decomposed by two domains, representing in temporal and sensor frequency [50] patterns, which are denoted as x^T and x^F , respectively. x^T is considered the same as x_i since the time series sensor data is entered in time sequence format. The symbols T and F also apply to augmented samples. The features of x^T and x^F are denoted as z^T and z^F , respectively.

3.3 Problem Definition

Given the sensor-based time series dataset \mathcal{X} with N samples, the objective of CLAN is to model *Encoders* from $p(x)$ for extracting invariant representations and a *Novelty Detector* which uses these representations to detect if x_{test} belongs to $p(x)$ or not.

\mathcal{X} lacks data regarding new activities since it is impossible to obtain information about new activities in advance in real-life scenarios. Consequently, the overall representation learning and novelty detection phases are designed without any new activity labels. Consistent with many previous studies, a high score from a score function of the novelty detector signifies that the given x_{test} is generated from the distribution $p(x)$.

4 CLAN: TWO-TOWER CONTRASTIVE LEARNING WITH DIVERSE DATA AUGMENTATION BASED NOVELTY DETECTION FRAMEWORK

This section provides an in-depth look at CLAN's extensive structure and its detailed modules, as illustrated in Figure 3. The initial step involves the preprocessing of raw sensor data using techniques commonly applied in HAR (Section 4.1). Subsequently, positives and negatives for each sample are generated by a variety of data augmentation techniques determined by the *Selector* (Section 4.2). From this data augmentation module, CLAN operates within a two-tower structure consisting of a time tower and a frequency tower. In each tower, CLAN's *Encoders* learn invariant representations for a known activity by contrasting an original sample with its diverse augmented samples and classifying the shift type of each augmented sample (Section 4.3). Finally, the *Novelty Detector* determines whether a given sample corresponds to a new activity by computing a score function based on its similarity to the learned representations and its likelihood of belonging to a known activity (Section 4.4).

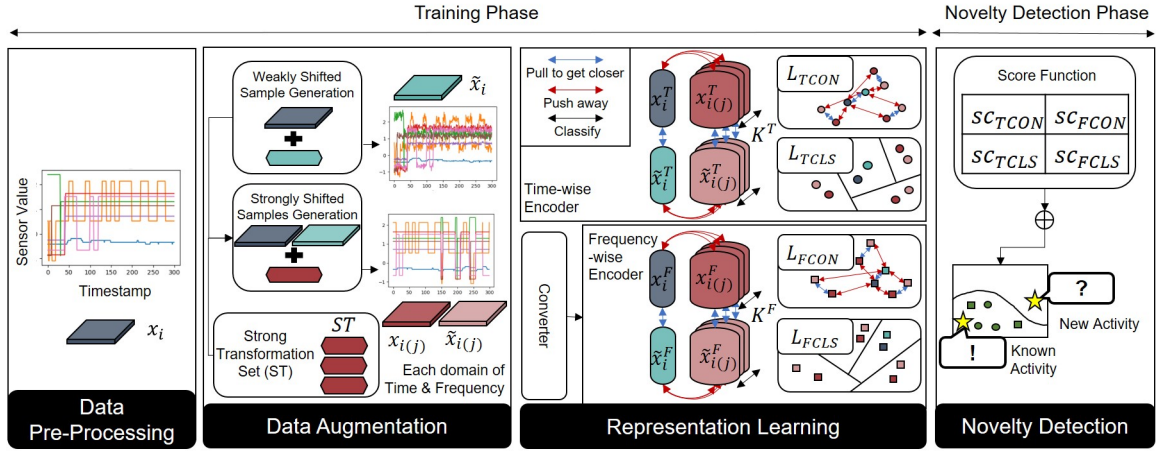


Fig. 3. A description of overview and components of CLAN. This is a simplified figure for visual understanding; the detailed formulas are written in Section 4.

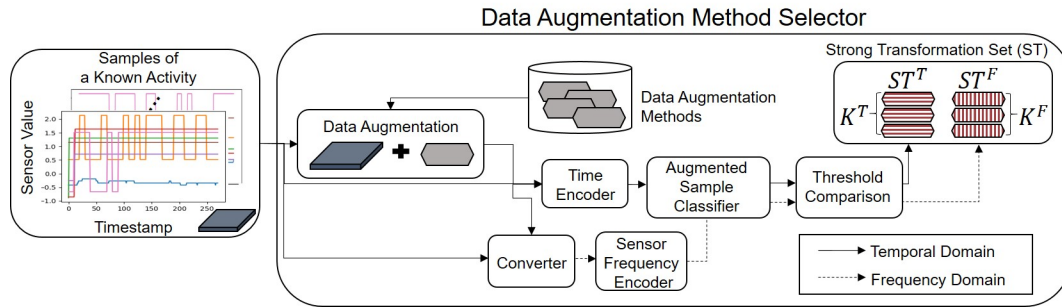


Fig. 4. Illustration of the overall process of determining data augmentation methods to construct ST for each dataset. This is a simplified figure for visual understanding; the detailed formulas are written in Section 4.2.

4.1 Data Pre-processing Module

In the initial stage, the collected raw sensor data derived from user actions undergoes preprocessing procedures as required. The data preprocessing module leverages widely used techniques in signal processing and HAR fields, such as signal smoothing, sensor value quantization, and data normalization [32, 55, 69]. The refined training dataset denoted as $\mathcal{X} \in \mathbb{R}^{N \times D \times L}$ is prepared.

4.2 Data Augmentation Module

4.2.1 Selecting Data Augmentation Methods. To apply various strongly shifted samples to contrastive learning of time series sensor data, we first establish the Strong Transformation family ST , a set of data augmentation methods for generating diverse types of negatives. The overall process of obtaining ST for each activity of each dataset is shown in Figure 4.

For a given training sample x , a specific data augmentation method \mathcal{T} is employed to produce an augmented sample denoted as $\mathcal{T}(x)$. The purpose of this module of CLAN is to calculate the classification performance

between x and $\mathcal{T}(x)$ to determine how much the $\mathcal{T}(x)$ changes from x in this module. Due to the varying degrees of shift in the time and frequency domains for each augmentation method, the degree of shift is measured separately for each domain. In the time domain, both x and $\mathcal{T}(x)$ are passed through the time encoder g_{ψ}^T , resulting in features $s^T = R_L(g_{\psi}^T(x))$ and $ts^T = R_L(g_{\psi}^T(\mathcal{T}(x)))$. In the frequency domain, the frequency conversion technique such as Fast Fourier Transform (FFT) is applied to x and $\mathcal{T}(x)$. We leverage the Fast Fourier Transformation (FFT) method [56] here due to its generality and efficiency. The resulting $FFT(x)$ and $FFT(\mathcal{T}(x))$ enter to the frequency encoder g_{ψ}^F , yielding features $s^F = R_L(g_{\psi}^F(FFT(x)))$ and $ts^F = R_L(g_{\psi}^F(FFT(\mathcal{T}(x))))$. It's important to note that the g_{ψ}^T and g_{ψ}^F are shared the architecture of the subsequent Transformer encoders used in contrastive learning (see Section 4.3.5) and we add one linear layer R_L for classification in here. ψ is parameters that are trained on each of g_{ψ}^T and g_{ψ}^F .

Due to the latter process being the same, we collectively refer to s^T and s^F as s , ts^T and ts^F as ts and g_{ψ}^T and g_{ψ}^F as g_{ψ} to simplify the terms. Each encoder learns ts and s , which is a binary classification problem, and the training objective function is defined as follows:

$$\mathcal{L}_{Aug_CLS} = -\frac{1}{2N} \sum_{i=1}^N [\log(p(ts_i)) + \log(1 - p(s_i))] \quad (1)$$

where \mathcal{L}_{Aug_CLS} represents a type of binary cross entropy loss (BCE) and $p(ts_i)$ and $p(s_i)$ are extracted from the sigmoid function [33] which is a function suitable for probability modeling that maps any real number of values to a value between 0 and 1.

Then, a simple classifier with g_{ψ} classifies s and ts , and derives the resulting classification performance $\alpha_{\mathcal{T}}$, which indicates how much $\mathcal{T}(x)$ is transformed from x . A high value of $\alpha_{\mathcal{T}}$ indicates a substantial dissimilarity between x and $\mathcal{T}(x)$, thereby signifying \mathcal{T} as a promising candidate to use as one of ST . Based on this rationale, we build a selector f_{θ} that uses $\alpha_{\mathcal{T}}$ to construct ST within a variety of data augmentation methods, as expressed by the following:

$$f_{\theta}(s, ts, \mathcal{T}) = ST \leftarrow \mathcal{T} \quad \text{if} \quad \alpha_{\mathcal{T}} \geq \theta_{ST} \quad (2)$$

Where θ_{ST} represents the threshold to determine whether to classify \mathcal{T} as one of ST . In the closed-set of data augmentation types, as the value of θ_{ST} increases, the number of available augmentation methods becomes more limited but they generate strongly shifted samples. Conversely, if the value of θ_{ST} is small, more augmentation methods can be selected, but this tends to produce less strongly shifted samples and increase computation time. Given that the specific requirements for each dataset and activity type vary, we employ an adaptive approach to construct an appropriate ST by flexibly adjusting θ_{ST} .

Table 1. AUROC (%) performance result for classifying the original sample and the augmented sample by each data augmentation method. The parentheses indicate specific activity class numbers within each dataset. A description of each data augmentation method is explained in Appendix C and the classification performance results of every activity for all datasets are shown in Appendix E.

Dataset	AddNoise	Reverse	Convolve	Scale (F)
DOO-RE (4)	50.0	97.2	51.1	96.6
CASAS (8)	50.2	98.1	93.9	97.8
OPPORTUNITY (5)	50.0	100.0	96.9	100.0
ARAS (16)	50.3	99.5	93.5	98.9

It is worth noting that even if the same data augmentation method is applied, the degree of shift depends on the dataset or activity types, as demonstrated in Table 1. Finally, ST is derived and stored for later use in the representation learning module, factoring in considerations related to the dataset, activity class, and domain (time or frequency).

4.2.2 Generating Positives and Negatives. Diverse types of shifted samples are generated through the application of K distinct data augmentation methods within the set ST . If multiple augmentation methods are used to generate strongly shifted samples, they are numbered to differentiate them. For example, if we choose \mathcal{T}_1 and \mathcal{T}_2 from ST , the resulting augmented samples from x are denoted as $x_{(1)}$ and $x_{(2)}$. Drawing insights from prior research [12, 73] and our own experimental findings in Section 5.3.1, we observe that employing a single data augmentation method for generating a positive of each x is typically sufficient. We create a positive sample \tilde{x} using the data augmentation technique with the lowest $\alpha_{\mathcal{T}}$ value.

4.3 Representation Learning Module

4.3.1 Contrastive Loss. In this section, we explain common definitions of contrastive learning with generalized terms. The main idea of contrastive learning, which operates on the principle of instance discrimination [80], is to learn the encoder g_ϕ by distinguishing similar views from others to obtain invariant representations of each class. ϕ is trainable parameters of the g_ϕ . The NT-Xent contrastive loss [15, 73] is utilized which is popularly used in contrastive learning, defined as follows:

$$\mathcal{L}_{con}(z, \{z^+\}, \{z^-\}) = -\frac{1}{|\{z^+\}|} \log \left(\frac{\sum_{z' \in \{z^+\}} \exp(\text{sim}(z, z')/\tau)}{\sum_{z' \in \{z^+\} \cup \{z^-\}} \exp(\text{sim}(z, z')/\tau)} \right) \quad (3)$$

where $z = g_\phi(x)$ and $z' = g_\phi(x')$ are the features of two data samples from the encoder g_ϕ . $\text{sim}(z, z') = z \cdot z' / \|z\| \|z'\|$ is a cosine similarity function that measures the similarity of the two samples. It maximizes the similarity between positive pairs and minimizes negative pairs. For a given input z , $\{z^+\}$ is a set of positive samples, and $\{z^-\}$ are negative samples. τ is the temperature parameter, a positive scalar that scales the similarity scores. $|\{z^+\}|$ indicates the cardinality of the set $\{z^+\}$.

4.3.2 Contrastive Learning for Encoders. Leveraging the above contrastive learning, we design a contrastive loss function that adapts to K number of augmented samples to learn invariant representations in CLAN's time and frequency encoders. In the latent space, the loss function encourages x and \tilde{x} to be in close proximity while simultaneously enforcing clear separations between x and \tilde{x} , and their augmented samples $x_{(j)} = \mathcal{T}_j(x)$ and $\tilde{x}_{(j)} = \mathcal{T}_j(\tilde{x})$, which are generated from $ST = \{\mathcal{T}_1, \dots, \mathcal{T}_j, \dots, \mathcal{T}_K\}$. Furthermore, any samples generated from other samples are still treated as negatives and are pushed away. Notably, $x_{(j)}$ and $\tilde{x}_{(j)}$ should be closer to each other than to other samples, so they also attract each other.

When applying the j -th data augmentation method to the i -th sample, we pass the input $x_{i(j)}$ and its corresponding positive sample $\tilde{x}_{i(j)}$ through a contrastive encoder g_ϕ (refer to Section 4.3.5). A projection layer is added on top of the encoder g_ϕ to extract features, yielding $z_{i(j)} = R_p(g_\phi(x_{i(j)}))$ and $\tilde{z}_{i(j)} = R_p(g_\phi(\tilde{x}_{i(j)}))$. To simplify terms, we define $\mathcal{T}_0 = I$ (*Identity*) (the identity data transformation method), resulting in $z_{i(0)} = z_i$ and $\tilde{z}_{i(0)} = \tilde{z}_i$. We then define a contrastive loss function that adapts to the number of K for the encoders used in CLAN as follows:

$$\mathcal{L}_{CON}(Z, ST) = \frac{1}{B} \frac{1}{K} \sum_{j=0}^K \sum_{i=1}^B \mathcal{L}_{con}(z_{i(j)}, \tilde{z}_{i(j)}, \{z_{i(j)}^-\}) \quad (4)$$

$$\text{where, } \{z_{i(j)}^-\} = \left\{ \left\{ \{z_{i(j)} \cup \tilde{z}_{i(j)}\}_{i=1}^B \right\}_{j=0}^K \right\} - \{z_{i(j)}, \tilde{z}_{i(j)}\}$$

where \mathcal{L}_{con} refers to the Equation (3), B corresponds to the batch size, Z indicates $\{z_i \cup \tilde{z}_i\}_{i=1}^B$, and K refers to the total number of data augmentation methods within ST . The pair $(z_{i(j)}, \tilde{z}_{i(j)})$ is used to denote a positive pair, with all remaining pairs being considered as negative pairs.

In addition to employing contrastive learning techniques, we incorporate an auxiliary classifier [36, 73] to enhance discriminative representation learning between strongly shifted samples. This task is to categorize the specific data augmentation method applied to each shifted sample. A linear layer is added on top of the encoder g_ϕ and extract features $s_{i(j)} = R_L(g_\phi(x_{i(j)}))$ and $\tilde{s}_{i(j)} = R_L(g_\phi(\tilde{x}_{i(j)}))$. The corresponding categorical cross-entropy loss function for classifying $K+1$ types (+1 for the original sample or weakly shifted sample) of shift is defined as follows:

$$\mathcal{L}_{CLS}(S, ST) = -\frac{1}{2B} \frac{1}{K} \sum_{j=0}^K \sum_{i=1}^B \left(\log(s_{i(j)}^j) + \log(\tilde{s}_{i(j)}^j) \right) \quad (5)$$

where $s_{i(j)}^j$ implies the predicted likelihood that $x_{i(j)}$ sample belongs to j -th data augmentation type in ST . S indicates $\{s_i \cup \tilde{s}_i\}_{i=1}^B$.

CLAN adopts a dual-loss approach that combines contrastive learning and auxiliary classification to capture the invariant representations resilient to diverse of variations in activity dynamics. Both loss terms, \mathcal{L}_{CON} and \mathcal{L}_{CLS} , are applied separately to the *Time-wise Encoder* and *Sensor Frequency-wise Encoder*, respectively.

4.3.3 Time-wise Encoder. To extract invariant representations that encompass temporal dependencies and intricate temporal dynamics information, we create a time-wise encoder $g_\phi^T(x)$. For a given training dataset \mathcal{X} , each individual sample, $x_i^T = x_i \in \mathcal{X}$ typically adheres to a time-sequential format as elucidated in Section 3. The loss functions intended for application to the time-wise encoder are adjusted as follows:

$$\mathcal{L}_{TCON} = \mathcal{L}_{CON}(Z \leftarrow \{z_i^T \cup \tilde{z}_i^T\}_{i=1}^B, ST \leftarrow ST^T) \quad (6)$$

where \mathcal{L}_{CON} is a contrastive loss function using Equation (4), z_i^T and \tilde{z}_i^T are features from $g_\phi^T(x_i^T)$ and $g_\phi^T(\tilde{x}_i^T)$ with a projection layer. The (z_i^T, \tilde{z}_i^T) signifies the positive pair, while the remaining pairs denote negative pairs. ST^T is a family of data augmentation methods that generate negatives when viewed from the temporal domain.

$$\mathcal{L}_{TCLS} = \mathcal{L}_{CLS}(S \leftarrow \{s_i^T \cup \tilde{s}_i^T\}_{i=1}^B, ST \leftarrow ST^T) \quad (7)$$

where \mathcal{L}_{CLS} is derived from Equation (5), and s_i^T and \tilde{s}_i^T are obtained from the time-wise encoder $g_\phi^T(x_i^T)$ and $g_\phi^T(\tilde{x}_i^T)$ through a linear layer.

The final objective function for learning invariant representations in the time encoder $g_\phi^T(x)$ is a combination of the Equation (6) and Equation (7):

$$\mathcal{L}_T = \mathcal{L}_{TCON} + \mathcal{L}_{TCLS} \quad (8)$$

\mathcal{L}_T is used to guide the learning of time-wise invariant representations for a known activity.

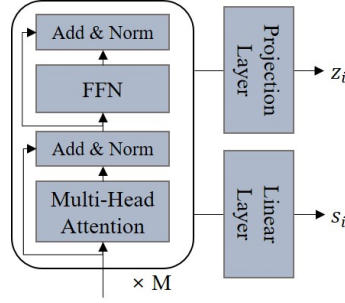


Fig. 5. The illustrative architecture of a Transformer encoder. The encoder effectively extracts invariant representations from time series sensor data using a multi-head attention and feedforward network with various abilities such as capturing complex time dependencies, handling variable length sequences, modeling critical frequency domain features, etc.

4.3.4 Sensor Frequency-wise Encoder. Recent research [71, 85, 86] underscores the significance of incorporating sensor frequency domain analysis in the representation of time series sensor data. Any technique that decomposes the data into time and frequency domains [11, 35, 50, 56, 60] is applicable to CLAN and we use the Fast Fourier Transformation (FFT) method [56] here due to its generality and efficiency. With the FFT, we extract the sensor frequency domain of a given sample, denoted as $x_i^F = FFT(x_i)$.

The subsequent step resembles the principles of contrastive learning and classification in the time-wise encoder. The contrastive and classification loss for the sensor frequency-wise encoder is computed as follows:

$$\mathcal{L}_{FCON} = \mathcal{L}_{CON}(Z \leftarrow \{z_i^F \cup \tilde{z}_i^F\}_{i=1}^B, ST \leftarrow ST^F) \quad (9)$$

where z_i^F and \tilde{z}_i^F are features obtained from $g_\phi^F(x_i^F)$ and $g_\phi^F(\tilde{x}_i^F)$ with the inclusion of a projection layer. ST^F is ST viewed from the frequency domain.

$$\mathcal{L}_{FCLS} = \mathcal{L}_{CLS}(S \leftarrow \{s_i^F \cup \tilde{s}_i^F\}_{i=1}^B, ST \leftarrow ST^F) \quad (10)$$

where s_i^F and \tilde{s}_i^F are obtained from $g_\phi^F(x_i^F)$ and $g_\phi^F(\tilde{x}_i^F)$ through a linear layer.

Similar to the time-wise encoder, we combine the Equation (9) and (10) to construct training objectives for the sensor frequency-side encoder g_ϕ^F as follows:

$$\mathcal{L}_F = \mathcal{L}_{FCON} + \mathcal{L}_{FCLS} \quad (11)$$

\mathcal{L}_F is used to guide the learning of invariant representations for known activities in the sensor frequency aspect.

4.3.5 Encoder Architecture. Recent advancements in the HAR field [26, 44, 45, 47, 49, 72, 79, 84] have showcased the efficacy of Transformer [75]-based methods inspired by NLP tasks. The Transformer offers advantages in both the temporal and frequency aspects of time series sensor data, including the ability to capture complex temporal dependencies, handle variable-length sequences, model important time and frequency domain features, and offer robustness to noise, making it suitable for a wide range of time series tasks. Therefore, we leverage the Transformer encoder architecture to g_ϕ and g_ψ , encoders with autoencoding characteristics.

As illustrated in Figure 5, the fundamental components of the Transformer encoder architecture encompass input embedding, and self-attention mechanisms designed to capture global interactions and correlations among D sensors within a given sample x . It employs multi-head attention for the simultaneous integration of richer information across various segments of the time series sequence, feed-forward neural networks (FFN) for feature

extraction and introducing non-linearity, residual connections and normalization to address issues related to gradient vanishing/exploding. The encoder stack with M layers to capture complex patterns and dependencies of time series sensor data.

We incorporate two distinct output layers on the top of the Transformer encoder: the projection layer R_P , responsible for extracting representations z_i to facilitate contrastive learning, and the linear layer R_L , tasked with extracting representations s_i for classification tasks.

4.3.6 Training Procedure. The overall training procedure of CLAN follows as described in Figure 3 with the proposed objective functions. $g_\phi^T(x)$ and $g_\phi^F(x)$ learns independently with no shared parameters. The final loss function for CLAN using Equation (8) and Equation (11) is formulated as:

$$\mathcal{L}_{CLAN} = \mathcal{L}_T + \beta \cdot \mathcal{L}_F \quad (12)$$

where β is a binary parameter (0 or 1) used to decide whether to use the frequency-side representation. \mathcal{L}_T and \mathcal{L}_F distinguish representations between known activity samples and their strongly shifted samples in temporal and frequency aspects, respectively.

4.4 Novelty Detection Module

For novelty detection using the learned invariant representations from the training procedure, we apply two types of score functions that correspond to each type of invariant representation.

Using invariant representation from contrastive learning (refer to Equation (4)), given a sample x , CLAN constructs features $z = R_P(g_\phi(x))$. A feature of a strongly shifted sample applying the j -th data augmentation method to x is $z_{(j)} = R_P(g_\phi(x_{(j)}))$. We exploit the cosine similarity between z and its nearest training sample z_{near} . In addition, the norm of the feature representation plays a crucial role in identifying novel class samples when using the SimCLR representation [15]. Referring to the experiment of previous work [73], the contrastive loss tends to result in a larger norm for the known class's samples as compared to the new class's samples. Among the training samples in \mathcal{X} , a sample with the highest similarity value with z is z_{near} . The score function is formulated as follows:

$$sc_{CON}(x) = \sum_{j=0}^K \lambda_{CON(j)} \cdot sim(z_{(j)}, z_{near,(j)}) \cdot \|z_{(j)}\| \quad (13)$$

where $\lambda_{CON(j)} = N / \sum_{i=1}^N sim(z_{i(j)}, z_{near,i(j)}) \cdot \|z_{i(j)}\|$ implies the importance weight of the j -th data augmentation method obtained from the training samples.

Additionally, CLAN also has a score function that utilizes representations from classifying (Equation (5)). CLAN transform x to $s = R_L(g_\phi(x))$, $x_{(j)}$ to $s_{(j)} = R_L(g_\phi(x_{(j)}))$ and a score function is represented as follows:

$$sc_{CLS}(x) = \sum_{j=0}^K \lambda_{CLS(j)} \cdot s_{(j)}^j \quad (14)$$

where $s_{(j)}^j$ implies the classification score that $x_{(j)}$ sample is classified as j -th data augmentation type in ST . $\lambda_{CLS(j)} = N / \sum_{i=1}^N s_{i(j)}^j$ is classification score based importance weight as similar to $\lambda_{CON(j)}$.

We apply the Equation (13) and (14) on both the temporal aspect and the sensor frequency domain, respectively. If x_{test} is coming in the novelty detection phase, x_{test} is decomposed as x_{test}^T and x_{test}^F as do in the training phase. The final score function for novelty detection is formulated as follows:

$$sc_{CLAN} = (sc_{CON}(x_{test}^T) + sc_{CLS}(x_{test}^T)) + \beta \cdot (sc_{CON}(x_{test}^F) + sc_{CLS}(x_{test}^F)) \quad (15)$$

where β is the same value used in Equation (12). The higher the value of sc_{CLAN} , the more likely it is that the corresponding x_{test} belongs to a known activity.

5 EXPERIMENTS AND EVALUATION

To evaluate CLAN’s performance, we conduct comparative experiments involving seven state-of-the-art approaches across four distinct real-world human activity datasets. Furthermore, diverse data augmentation impact tests are evaluated, and ablation studies are carried out to scrutinize the effectiveness of the proposed components. The following research questions are addressed through the experiments:

- **Q1.** *Can CLAN outperform state-of-the-art approaches to detect novelty in HAR?* (Section 5.2)
- **Q2.** *How effective is CLAN’s strategy of applying diverse strongly shifted samples as negatives?* (Section 5.3)
- **Q3.** *How effective are multifaceted (temporal, frequency) distinctive representations in distinguishing between known and new activities?* (Section 5.4)
- **Q4.** *Is CLAN sensitive to parameter variations?* (Section 5.5)
- **Q5.** *Is CLAN suitable for application in real-world scenarios?* (Appendix K, L)

5.1 Experiment Setup

This section covers the datasets and evaluation metrics used in the experiments. The details of baselines in novelty detection are described in Appendix B, and implementation details are explained in Appendix D.

5.1.1 Datasets. The real world involves a broad spectrum of activities, from simple activities such as *a user standing up* to complex activities such as *users having a meeting*. To assess the effectiveness of CLAN in various AAL environments, we select four datasets, each exhibiting distinct characteristics as shown in Figure 6.

DOO-RE Dataset¹ [43] comprises data collected from ambient sensors in a university seminar room, with a minimum of three participants in 4 different group activity. The dataset is based on 7 types of ambient sensor states, including *Seat occupation*, *Sound level*, *Brightness level*, *Light status*, *Existence status*, *Projector status*, and *Presenter detection status*. The dataset contains the sensor information including timestamp, sensor type, and sensor state. In total, the dataset consists of 340 activity episodes.

¹<http://doo-re.kaist.ac.kr/>

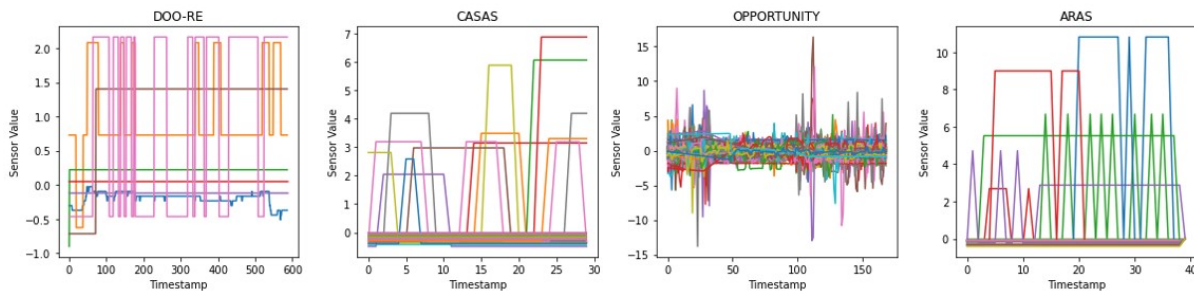


Fig. 6. Visualization of samples for each dataset. The x-axis of each graph is timestamps and the y-axis represents normalized sensor values. *DOO-RE* encompasses ambient sensor data in a multi-user setting, *CASAS* includes motion sensor-oriented data in a two-user environment, *OPPORTUNITY* comprises a combination of wearable and ambient sensor data collected from a single user, and *ARAS* includes data collected from diverse ambient sensors in a two-user environment.

CASAS Dataset² [70] consists of a trio of ambient sensor types deployed within a smart home environment tailored for 14 distinct types of multi-user activities. The data is collected by 51 *motion* sensors, 2 *item* sensors, and 8 *door* sensors, which implies that the main purpose of the dataset is to track user movements. These sensors record data about their activation, including the specific sensor type, the date, and the timestamp. This dataset consists of a total of 469 activity samples.

OPPORTUNITY Dataset³ [62] is a dataset designed for the recognition of 5 daily activities of 4 single users, leveraging wearable and ambient sensors. It includes state change data of various 242 sensor types, such as *Switches* and *3D acceleration sensors in drawers*, using a sampling rate of 1 Hz for all sensors. The dataset captures the state of all sensors at every timestamp for each activity sample. The dataset includes a total of 120 samples of the activities.

ARAS Dataset⁴ [5] is an ambient sensor-based dataset originating from 16 simple activities in a smart home with multiple residents. The smart home is equipped with 20 types of ambient sensors, such as *Door* and *Chair* sensors. The dataset provides data that records the state of each sensor in binary form at every timestamp. The dataset consists of a total of 3,088 activity samples.

To alleviate privacy concerns and simulate real-world situations, all user-identifiable information has been excluded. Details about the activities and sensor types within each dataset are described in Appendix A.

5.1.2 Evaluation Metrics. To comprehensively assess the effectiveness of CLAN in different aspects, we select three commonly used metrics for evaluating novelty detection performance. We utilize two broad-scale evaluation metrics, namely **AUROC** and **Balanced Accuracy**, and a finer-scale metric, **FPR@TPR0.95**. The terms positive and negative used in this section are common terms used in the performance metrics. Samples from the new activity are considered positive and samples from the known activity are considered negative.

Area Under the Receiver Operating Characteristic curve (AUROC) provides a comprehensive overview of the model's ability to distinguish between known and new activity samples across different detection thresholds. It quantifies the trade-off between true positive rates and false positive rates.

Balanced Accuracy [8] provides an average accuracy against data imbalance, providing a balanced assessment of the detection performance of each known and new activity class. The formula for Balanced Accuracy is:

$$\begin{aligned} \text{Sensitivity (Recall)} &= \frac{\text{True Positives}}{\text{True Positives} + \text{False Negatives}} \\ \text{Specificity} &= \frac{\text{True Negatives}}{\text{True Negatives} + \text{False Positives}} \\ \text{Balanced Accuracy} &= \frac{\text{Sensitivity} + \text{Specificity}}{2} \end{aligned}$$

For measuring the accuracy, the predicted label for each sample is determined based on its novelty detection score. The number of known activity samples out of the total number of test samples is calculated as a percentage, and the value corresponding to the percentage of the novelty detection scores of the total samples is set as the threshold for determining the prediction label for each sample.

False Positive Rate at True Positive Rate 0.95 (FPR@TPR 0.95) measures the rate of false positives while maintaining a fixed true positive rate of 0.95. This metric clearly shows numerically how many of the known activity samples are incorrectly detected as new when 95% of the new activity samples are correctly detected.

In the following sections, we use **ACC** to denote Balanced Accuracy, and **FPR** to denote FPR@TPR 0.95. Higher values of AUROC and ACC indicate better performance, while lower values of FPR signify better performance.

²<https://casas.wsu.edu/datasets/>

³<https://archive.ics.uci.edu/ml/datasets/opportunity+activity+recognition>

⁴<https://www.cmpe.boun.edu.tr/aras/>

Table 2. Performance comparison of CLAN and baselines in one-class and unsupervised setups for all datasets. The experimental results are the mean and standard deviation performance results of one-class classification tasks for all activities within each dataset. Each one-class classification task is performed in 10 trials. For each metric, the best-performing value is highlighted in bold and the second-best value is underlined.

Model	DOO-RE			CASAS			OPPORTUNITY			ARAS		
	AUROC ↑	ACC ↑	FPR ↓	AUROC ↑	ACC ↑	FPR ↓	AUROC ↑	ACC ↑	FPR ↓	AUROC ↑	ACC ↑	FPR ↓
OC-SVM	50.2	50.1	94.6	80.8	67.9	57.4	82.5	71.8	54.9	72.0	59.2	73.4
DeepSVDD	±2.3	±1.5	±1.9	±14.7	±13.0	±27.8	±2.0	±1.5	±6.8	±7.8	±6.5	±15.1
	62.6	60.6	83.1	63.4	60.3	73.3	86.1	81.9	30.9	68.3	59.7	72.6
AE	±4.4	±1.2	±4.5	±18.8	±9.3	±20.2	±2.4	±2.2	±4.7	±12.7	±4.8	±11.6
	76.8	66.7	56.8	55.7	51.6	84.1	62.2	55.2	65.9	57.9	51.0	84.7
OCGAN	±10.3	±12.0	±21.0	±18.8	±6.6	±19.3	±21.7	±20.2	±29.0	±11.9	±2.6	±11.2
	77.9	67.8	58.2	60.6	53.8	82.3	61.5	53.3	65.7	60.1	52.0	84.2
SimCLR	±6.2	±6.3	±17.4	±19.3	±8.0	±20.3	±20.7	±20.5	±30.2	±12.2	±3.5	±11.6
	63.6	61.7	71.0	58.3	60.0	75.1	<u>90.7</u>	<u>87.7</u>	36.8	77.7	<u>69.6</u>	56.5
GOAD	±12.3	±8.5	±17.0	±13.0	±6.6	±17.9	±2.7	±5.6	±9.3	±7.3	±5.4	±15.1
	71.5	64.5	60.7	78.9	66.0	62.3	63.0	60.1	77.9	<u>84.8</u>	66.7	51.8
FewSome	±5.8	±5.4	±6.0	±7.1	±4.0	±12.6	±4.9	±4.2	±6.4	±5.3	±6.4	±13.5
	<u>91.4</u>	<u>83.0</u>	<u>33.3</u>	<u>91.1</u>	<u>79.5</u>	<u>32.5</u>	88.7	84.7	<u>25.8</u>	81.6	68.9	<u>51.1</u>
CLAN	±4.7	±4.4	±12.0	±6.3	±7.3	±16.7	±4.3	±5.6	±11.3	±9.2	±6.5	±16.2
	95.8	91.0	22.2	98.7	93.2	10.8	98.0	95.6	10.1	94.9	82.4	24.5
	±3.2	±5.2	±17.2	±1.5	±5.0	±9.5	±2.0	±3.8	±9.2	±4.8	±7.8	±18.5

5.2 Novelty Detection Performance Comparison (Q1)

In this section, we evaluate the general applicability of CLAN in HAR by analyzing the results of novelty detection performance in both single-class and multi-class configurations. Comparisons are made between CLAN and a range of novelty detection approaches, including One-class classification-based (*OC-SVM*, *DeepSVDD*), Reconstruction-based (*AE*, *OCGAN*), and Contrastive learning-based (*SimCLR*, *GOAD*, *FewSome*) approaches. Their details are explained in Appendix B.

5.2.1 One-class Setup. As done in all previous baselines, we conduct an experiment focusing on one-class classification to measure novelty detection performance. One activity is designated as the known activity, and the other activities are regarded as new activities. If there are C activities in the dataset, we perform C distinct one-class classification tasks.

Table 2 illustrates that in one-class classification scenarios, CLAN outperforms other methods in identifying novel patterns across various datasets. Specifically, CLAN improves the AUROC by margins of 4.8% for the DOO-RE; 8.4% for CASAS; 8.0% for OPPORTUNITY; and 12.0% for ARAS, respectively, surpassing the best results from the baselines. Unlike these baselines, which exhibit significant performance variability across datasets, CLAN maintains consistently high performance, exceeding 90% across all types of datasets. This consistent performance suggests that the mechanisms incorporated into CLAN, which take into account the properties of time series sensor data, successfully extract invariant representations applicable to all datasets, demonstrating its generalization ability in detecting novelties.

In general, approaches using contrastive learning outperform other methods. This demonstrates that employing contrast mechanisms for instance discrimination [80] is a potent strategy for identifying new patterns in time series sensor data. Contrastive learning enables the generation of key representations, even in the presence of temporal dynamics in time series sensor data. To delve deeper into the results, CLAN outshines other contrastive learning benchmarks across all metrics and datasets. CLAN, which considers the diversity of positives and

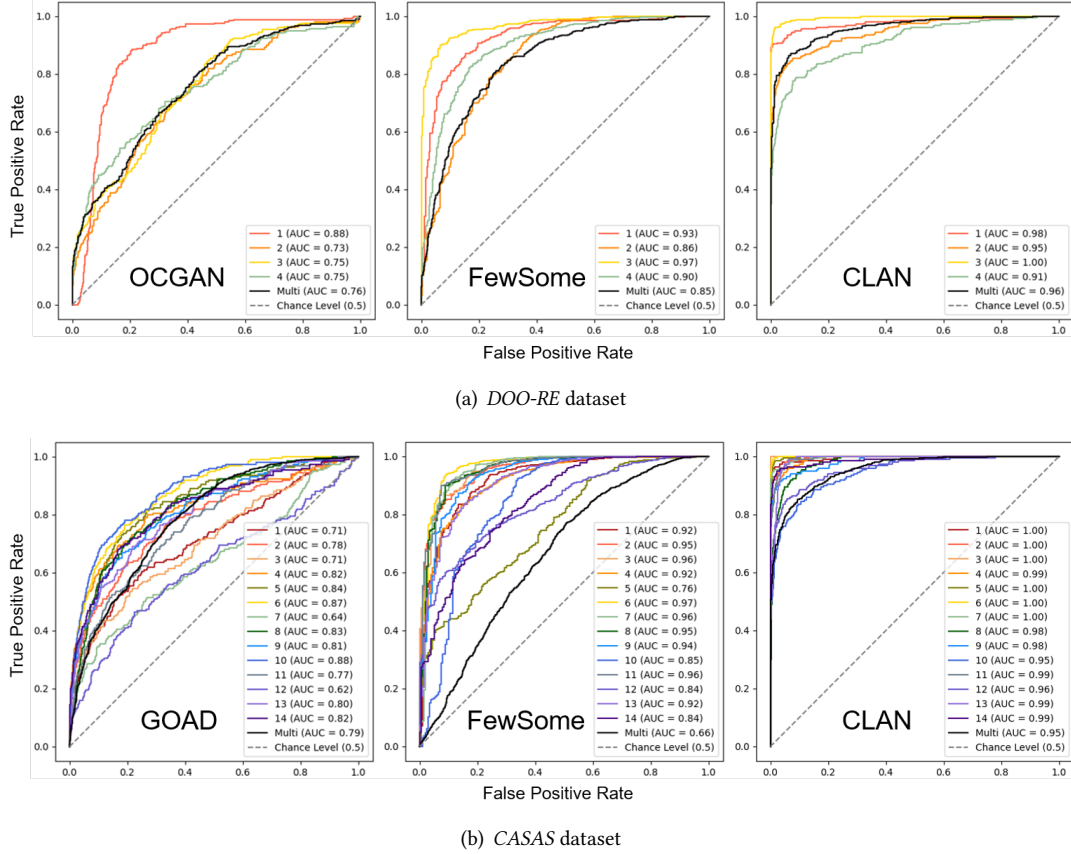


Fig. 7. ROC curve graphs for the *CASAS* and *DOO-RE* datasets. Roc curve graphs for *OPPORTUNITY* and *ARAS* are described in Appendix G. We draw figures of CLAN and two baselines that provide decent performance for each dataset. The positioning of the ROC graph closer to the top-left corner indicates superior performance. The numerical labels on each ROC curve graph correspond to the distinct activities in each dataset, as detailed in Appendix A. The value in parentheses next to each activity indicates the performance of one-class classification for that activity. ROC curves labeled as *Multi* display the mean performance across multi-class scenarios.

negatives in the multifaceted, yields more discriminatory activity representations than the other contrastive learning-based baselines that only focus on attracting positives.

CLAN enhances ACC and FPR by 9.7% and 33.1% for *DOO-RE*; 17.2% and 66.7% for *CASAS*; 9.1% and 60.9% for *OPPORTUNITY*; and 19.1% and 52.5% for *ARAS*, respectively, surpassing the best baseline performances. The advancement rates in ACC and FPR exceed those in AUROC. This indicates that CLAN achieves superior balanced performance in detecting both known and new activities compared to other baselines. It implies that CLAN effectively minimizes feature overlap between known and novel activities while generating invariant representations. Moreover, even in cases where there are common features, CLAN has the ability to distinguish between them through multi-faceted analysis.

Figure 7 illustrates the outstanding performance of CLAN in detail for each known activity, showcasing ROC curve graphs for both the *DOO-RE* and *CASAS* datasets. This demonstrates CLAN’s consistent excellence across all one-class classification tasks, not just on average. It shows CLAN functions to prevent some meaningless temporal dynamics or similar features between activities, for each type of known activity. For example, activities like *Studying together (2)* in *DOO-RE* and *Retrieve dishes from a kitchen cabinet (12)* in *CASAS*, which may share sound or motion features with other activities, are better represented by CLAN compared to baseline methods due to its superior discrimination capabilities.

Other baseline approaches exhibit significant performance variations depending on the type of activity, such as OCGAN with *Samll talk (1)* in *DOO-RE*, and GOAD with *Retrieve dishes from a kitchen cabinet (12)* and FewSome with *Sweep the kitchen floor (5)* in *CASAS*. However, CLAN maintains uniformly excellent performance across various activities, indicating its proficiency in deriving invariant representations tailored to each specific activity.

The figures also show how slowly the performance of the False Positive Rate (FPR) increases to increase the True Positive Rate (TPR). This indicates the extent to which the expressive capability of known activities is diminished to effectively highlight the core features of new activities. It’s demonstrated that the CLAN effectively balances the recognition of both known and novel activities by minimally diminishing the expressiveness of known activities.

5.2.2 Multi-class Setup. Inspired by the previous work [73], we perform an experiment in a multi-class setup in which multiple types of activity exist in both known and new activities. This setting mirrors real-world scenarios more closely. In structuring the multi-class setup, we divide the activities within the same dataset into two equal halves: one representing known activities and the other, new activities. We conduct 10 trials consisting of randomly selected known and novel activity sets and calculate the mean of the results. To ensure consistency of the sets of known and new activities for each trial across baselines and CLAN, fixed seeds are employed during the random selection process.

In Table 3, CLAN outperforms the highest baseline results, showing greater improvements in average AUROC, ACC, and FPR by margins of 14.3%, 16.7%, and 53.4% for *DOO-RE*; 15.6%, 14.6%, and 52.6% for *CASAS*; 6.3%, 9.7%,

Table 3. Performance comparison of CLAN and baselines in multi-class and unsupervised setups for all datasets. The experimental results are the mean and standard deviation performance results of 10 random multi-class settings. For each metric, the best-performing value is highlighted in bold and the second-best value is underlined.

Model	DOO-RE			CASAS			OPPORTUNITY			ARAS		
	AUROC ↑	ACC ↑	FPR ↓	AUROC ↑	ACC ↑	FPR ↓	AUROC ↑	ACC ↑	FPR ↓	AUROC ↑	ACC ↑	FPR ↓
OC-SVM	51.7	51.4	94.2	58.4	56.3	87.8	74.3	65.9	65.6	52.0	51.7	93.9
DeepSVDD	±3.4	±2.2	±3.7	±9.4	±6.2	±11.2	±4.5	±3.3	±8.6	±6.8	±4.7	±4.0
	64.1	61.0	85.6	69.8	64.3	87.3	88.6	79.3	<u>32.9</u>	53.2	52.2	93.7
AE	±13.8	±11.2	±9.4	±5.5	±4.1	±3.8	±3.6	±5.0	±8.7	±1.4	±1.0	±0.8
	67.2	64.6	76.2	54.4	53.4	94.1	52.2	54.7	94.4	51.3	51.1	93.2
OCGAN	±21.2	±18.0	±28.7	±9.4	±7.3	±4.2	±15.4	±11.2	±7.6	±6.0	±4.5	±4.2
	73.6	68.3	71.7	54.0	53.7	93.6	54.6	57.8	89.4	51.3	51.1	94.3
SimCLR	±16.7	±14.7	±22.3	±9.2	±7.0	±3.0	±12.7	±7.9	±11.5	±5.5	±4.3	±3.4
	73.8	67.7	63.5	82.3	<u>77.1</u>	<u>51.1</u>	92.9	<u>85.9</u>	38.8	<u>74.9</u>	<u>68.5</u>	<u>73.2</u>
GOAD	±18.8	±16.4	±24.3	±18.2	±16.8	±30.3	±6.3	±8.1	±31.6	±11.1	±9.3	±13.5
	71.4	63.5	67.3	<u>82.8</u>	75.8	56.1	53.5	52.6	90.9	68.1	63.0	76.9
FewSome	±13.1	±13.0	±23.0	±5.6	±4.9	±12.3	±10.6	±7.1	±13.7	±6.6	±5.1	±8.4
	<u>84.2</u>	<u>77.1</u>	<u>53.3</u>	66.2	61.4	79.2	68.4	60.9	71.7	56.4	54.4	89.6
CLAN	±6.8	±7.5	±16.6	±6.3	±6.2	±5.4	±8.2	±9.4	±11.5	±3.9	±2.3	±5.1
	96.3	90.0	24.8	95.7	88.4	24.2	98.8	94.3	6.3	77.9	71.5	70.3
	±2.8	±4.0	±17.2	±1.9	±3.2	±9.3	±1.8	±5.4	±11.9	±4.9	±4.0	±10.7

and 81.0% for *OPPORTUNITY*; and 3.9%, 4.4%, and 4.0% for *ARAS*. This demonstrates that CLAN significantly exceeds the performance of other methods across all datasets, mirroring its success in one-class scenarios. The ACC and FPR metrics indicate that the CLAN has a balanced identification ability of known and new activities. The superior performance of contrastive learning-based techniques, particularly CLAN, is credited to their ability to perform instance discrimination effectively on each sample when dealing with multiple known activities. Even in the multi-class setting, CLAN’s unique representations of known activities amid various temporal dynamics are key to its high performance.

Compared to other baselines, CLAN shows resilience in maintaining performance levels in the multi-class setup. This is evident in Figure 7, where FewSome’s effectiveness diminishes because of the growing similarity in features between known and new activities in multi-class configurations. CLAN, on the other hand, benefits from considering variations from individual samples in both time and frequency domains, leading to the development of superior invariant representations across multiple activities.

5.3 Effects of Diverse Data Augmentation (Q2)

In this experiment, we demonstrate that CLAN’s data augmentation mechanism, which generates positives and negatives for HAR, is effective through statistical analysis and an ablation study.

5.3.1 Correlation between $\alpha_{\mathcal{T}}$ and Novelty Detection Performance. For all datasets, we investigate the correlation between the shifted sample classification performance $\alpha_{\mathcal{T}}$ of a specific augmentation method \mathcal{T} and the final novelty detection performance. This determines whether data augmentation methods that significantly shift the original data actually have a valid effect on novelty detection performance. We obtain the value of each $\alpha_{\mathcal{T}}$ (Appendix E) for 10 different data augmentation techniques (Appendix C), and then assess the novelty detection performance when these methods are employed to generate negatives, as well as the performance when they are used to generate positives.

Table 4 provides the correlation results between these two factors utilizing correlation coefficients [4, 19]. *Weak* refers to the improvement in novelty detection performance when data augmentation techniques with lower values of $\alpha_{\mathcal{T}}$ are used to generate positives. *Strong* denotes the enhancement in novelty detection performance when data augmentation techniques with higher values of $\alpha_{\mathcal{T}}$ are chosen for generating negatives. The *Weak* results show coefficient values ranging from 0.1 to 0.3 (in a minus direction), implying that selecting data augmentations that weakly shift samples for generating positives has a limited impact on performance enhancement. Conversely, the *Strong* results exhibit coefficient values ranging from 0.4 to 0.6, along with very low p-values, indicating that selecting data augmentation methods that strongly shift samples for generating negatives significantly impacts novelty detection performance. These findings affirm the importance of selecting appropriate data augmentation methods that produce strong shifted samples to generate negatives. This underscores the significance of CLAN’s data augmentation selector in the overall performance. Following these experimental results, to select more data augmentation methods to increase the types of negatives, we design CLAN to select only one data augmentation method with the lowest $\alpha_{\mathcal{T}}$ to generate positives, and the rest contribute to *ST* configuration.

Table 4. Coefficient correlation [4, 19] values between $\alpha_{\mathcal{T}}$ and novelty detection performance. A coefficient value exceeding the absolute value of 0.4 signifies a meaningful correlation, and lower p-values indicate more significant relationships.

Dataset	DOO-RE	CASAS	OPPORTUNITY	ARAS	
Strong	0.618 ** ($< .001$)	0.511 ** ($< .001$)	0.670 ** ($< .001$)	0.480 ** ($< .001$)	<i>Note.</i> * $p < .05$, ** $p < .001$
Weak	- 0.215 * (0.042)	- 0.170 (0.108)	- 0.136 (0.203)	- 0.146 (0.170)	

Table 5. AUROC performance (%) for ablation study of CLAN’s diverse data augmentation strategy across all datasets. *Single* refers to applying only one type of data augmentation, *Multiple* refers to applying various types of data augmentation, *Random* indicates that data augmentation methods are chosen randomly, and *ST* symbolizes that the data augmentation methods are selected using a Strong Transformation Set. For each dataset, the best-performing value is highlighted in bold and the second-best value is underlined.

	Single	Multiple	Random	ST	DOO-RE	CASAS	OPPORTUNITY	ARAS	Mean
(a) - CLAN		✓		✓	95.8 ±3.2	98.7 ±1.5	98.0 ±2.0	94.9 ±4.8	96.9 ±1.8
(b)		✓	✓		86.4 ±8.9	92.5 ±5.8	95.6 ±3.0	88.8 ±8.2	90.8 ±4.1
(c)	✓			✓	<u>90.5</u> ±4.8	<u>95.1</u> ±2.6	<u>95.7</u> ±2.7	<u>89.0</u> ±5.7	<u>92.6</u> ±3.3
(d)	✓		✓		74.0 ±5.0	78.4 ±6.9	87.9 ±6.1	78.6 ±6.6	79.7 ±5.9
(e)					63.6 ±12.3	58.3 ±13.0	90.7 ±2.7	77.7 ±7.3	72.6 ±14.6

Table 6. AUROC performance (%) for ablation study of CLAN’s components on all datasets. It shows the effects of multifaceted representations. *TCON* and *TCLS* symbolize the use of contrastive learning and classification-based representations in the temporal domain. Similarly, *FCON* and *FCLS* mean using representations based on contrastive learning and classification in the frequency domain. For each dataset, the best-performing value is highlighted in bold and the second-best value is underlined.

	TCON	TCLS	FCON	FCLS	DOO-RE	CASAS	OPPORTUNITY	ARAS	Mean
ALL - CLAN	✓	✓	✓	✓	95.8 ±3.2	98.7 ±1.5	98.0 ±2.0	94.9 ±4.8	96.9 ±1.8
T	✓	✓			<u>94.4</u> ±6.7	95.0 ±4.6	97.6 ±2.9	91.7 ±5.5	<u>94.7</u> ±2.4
F			✓	✓	90.8 ±3.0	<u>97.3</u> ±2.4	96.5 ±2.3	91.6 ±7.3	94.1 ±3.3
CON	✓		✓		89.6 ±6.7	93.9 ±6.8	92.6 ±2.3	<u>93.9</u> ±6.7	92.5 ±2.0
CLS		✓		✓	94.0 ±6.7	94.5 ±4.7	<u>97.9</u> ±1.5	87.9 ±6.3	93.6 ±4.3

5.3.2 *Effects of Diverse Types of Strongly Shifted Samples.* We verify the impact on novelty detection performance when using strongly shifted samples as negatives, achieved through diverse data augmentation techniques, as illustrated in Table 5. In the ablation study, (a) represents the CLAN as it is, (b) describes the scenario where *ST* is not considered, (c) refers to cases where multiple types of data augmentation methods are not considered, (d) signifies the situation where both *ST* and multiple types of data augmentation methods are ignored, and (e) refers to when none of these factors are considered in creating negatives.

The CLAN derives the best performance on all datasets. The strategy of employing strongly shifted samples as negatives, attained via a variety of data augmentation methods, proves effective for the HAR field. CLAN surpasses (b) by 6.7% and (c) by 4.7%, respectively, indicating its ability to generate invariant representations that remain unbiased towards any variation, while still preserving the distinctive qualities of known activity. Observing that (c) outperforms (b) across all datasets suggests that the effectiveness of data augmentation lies more in the selection of appropriate types for generating negatives, rather than merely expanding the number of augmentation techniques. Comparing (d) with (b) or (c), either through quantitatively increasing the number of data augmentation methods or the qualitative improvement of negatives (*ST*) can greatly help improve novelty detection performance. This experiment concludes that qualitative or quantitative refinement of negatives greatly helps identify essential invariant representations of known activities. Extensive studies examining the impact of varying the quantity or quality of data augmentation techniques for negative generation are presented in Appendix H.

5.4 Ablation Study (Q3)

We conduct an ablation study to evaluate the impact of different components in CLAN across all datasets, as detailed in Table 6. The study involves four key aspects: **T** represents the novelty detection results when focusing solely on temporal characteristics, using TCON and TCLS losses for representation learning. **F** pertains to focusing exclusively on frequency characteristics for novelty detection, using FCON and FTLS losses for representation. **CON** examines the outcomes when employing only contrastive learning, utilizing TCON and FCON losses for learning representations. **CLS** analyzes the results when relying solely on classification loss, with representations learned through TCLS and FTLS losses.

The results show that CLAN’s novelty detection performance is superior by 2.3%, 3.0%, 4.7%, and 3.5% respectively, compared **T**, **F**, **CON** and **CLS**. This underscores the effectiveness of multi-faceted representations in novelty detection across different datasets. The contribution of those components to representation formation varies with each dataset. For instance, in *DOO-RE* and *OPPORTUNITY*, **T** outperforms **F**, while in *CASAS*, **F** surpasses **T**. This also happens within activities within the same dataset. For example, in *DOO-RE*, **F** yields better results for the *Seminar* activity, whereas **T** excels in *Technical Discussion*. This implies that the domains where significant features emerge might vary based on the traits of known activities. Consequently, CLAN that covers both these domains can be deployed more thoroughly and effectively across various activities. Notably, CLAN demonstrates robust performance in datasets with a wide range of activities, like *CASAS* and *ARAS*. Even if there are activities that have shared characteristics after temporal analysis additional information such as periodicity of movements and frequency of chair use can be obtained by analyzing the frequency aspect, allowing a better representation of known activities. Both **CON** and **CLS** contribute to creating invariant representations across all datasets. By integrating these two objectives, CLAN accurately derives key aspects of known activities without being influenced by meaningless temporal dynamics. Therefore, CLAN’s comprehensive approach of integrating all these factors to find invariant representations has proven to be practical and effective.

5.5 Parameter Sensitivity (Q4)

In this section, we conduct sensitivity analysis to explore how key parameters affect CLAN. This includes investigating the threshold θ_{ST} for data augmentation selection (Section 4.2), the temperature factor τ , and the batch size B used in contrastive learning (Section 4.3).

5.5.1 Threshold Value θ_{ST} . This section investigates how altering θ_{ST} (both θ_{ST}^T and θ_{ST}^F) in increments of 0.1, ranging from 0.5 to 0.9, affects the performance across all datasets. An increase in θ_{ST} results in retaining only the essential data augmentation methods that shift the data significantly, albeit reducing the overall number of applicable methods. Conversely, decreasing θ_{ST} leads to the opposite effects. As illustrated in Figure 8(a), performance tends to stay similar or improve with higher θ_{ST} values. A higher θ_{ST} favors focusing on key data augmentation methods, enhancing the generation of temporally irrelevant dynamics from original data, aiding in the extraction of invariant representations of known activities. In addition, a larger θ_{ST} also contributes to shorter inference times, as green bars indicated in Figure 8(a). Notably, when θ_{ST} is set to 0.9, the performance for *DOO-RE* declines, though it still surpasses other baselines. This is attributed to the limitation of having only one type of data augmentation for creating negatives of activities like *Studying together* or *Seminar*. This indicates that employing multiple data augmentation types leads to more robust representations than relying on a single method. Therefore, it is advisable to determine the highest feasible θ_{ST} that can obtain multiple augmentation methods to balance time efficiency and accuracy effectively. The boundary study on the impact of changing the quantity or quality of data augmentation techniques for negative generation is presented in Appendix H.

5.5.2 Temperature Factor τ . We assess how adjusting τ affects novelty detection in time series data, following the τ range defined in previous research [76]. The parameter τ plays a crucial role in determining the severity of

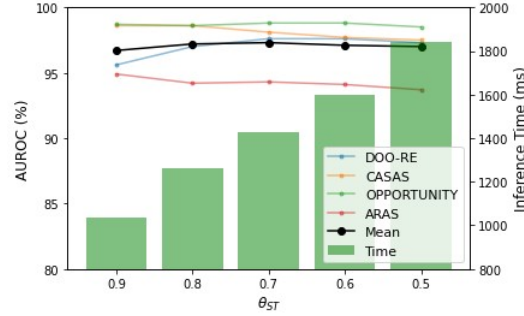
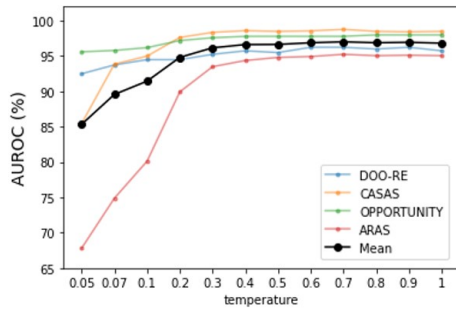
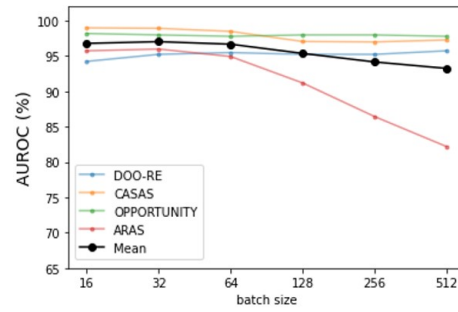
(a) Threshold θ_{ST} .(b) Temperature factor τ (c) Batch size B

Fig. 8. Exploring the effects of threshold (θ_{ST}) in data augmentation selection, and temperature factor (τ) and batch size (B) in contrastive learning: This graph illustrates how these parameters influence the novelty detection performance of CLAN. The x-axis shows the varying values of each parameter, while the y-axis indicates the performance results. Different dataset types are denoted by distinct colors, and a black plot marks the average performance across all datasets.

penalties applied to negative samples within contrastive learning. A smaller value of τ hinders the task of forming a broad representation structure in the latent space, as it tends to concentrate on the properties of individual samples. Conversely, a larger τ facilitates the learning of more general patterns but may neglect the intricate specifics of certain activities. The ideal adjustment of τ relies on the distinctive characteristics of each dataset. As depicted in Figure 8(b), the value of τ reaches stable points beyond 0.3 in all datasets. This observation leads to two key implications. 1) For effective construction of time series sensor data representations, it's more crucial to build generalized representations even at the cost of somewhat overlooking slight variations in some samples to address challenges such as noise and insignificant temporal fluctuations. 2) To effectively discern novelties in HAR, it's preferable to learn semantic structures in the latent space that encompass a wide spectrum of patterns, rather than focusing solely on specific interval patterns like individual or subsequence levels.

5.5.3 Batch Size B . In contrastive learning, batch size plays a crucial role in shaping representation learning by influencing the count of positive and negative samples for comparison. As the batch size grows, so does the number of samples for comparison, demanding more memory. Conversely, a smaller batch size results in fewer samples for comparison, which can extend training time. As demonstrated in 8(c), we experiment with various batch sizes, doubling them from 16 to 512 across all datasets. We observe that performance starts to decline

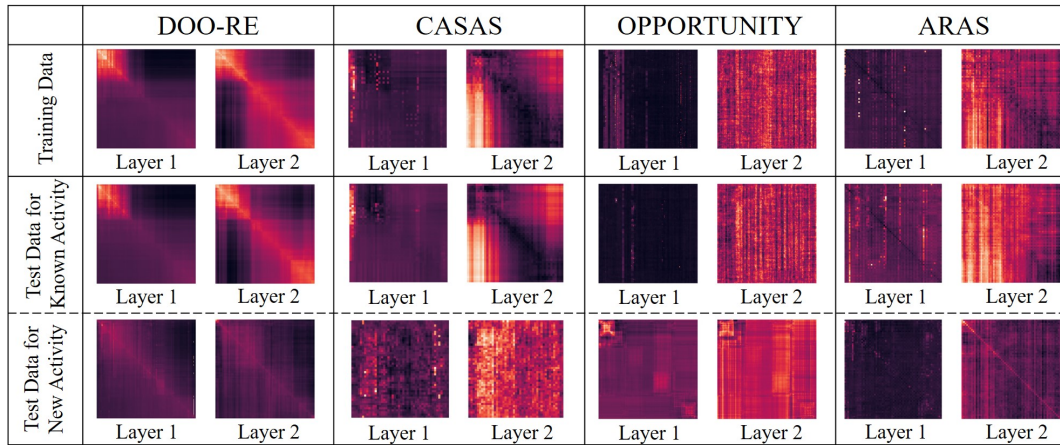


Fig. 9. Attention maps for each dataset of learned representations for known activities, representations for when the test data are a known activity, and when they are a new activity. The higher the attention weight, the brighter the color, and the lower the attention weight, the darker the color.

notably in *CASAS* and *ARAS* datasets when the batch size exceeds 64. This decline can be linked to the large variety of activity classes in these datasets, leading to a higher count of negative samples for comparison as batch size increases. As a result, the representations learned tend to prioritize distinguishing against negatives over capturing essential features of the known activity, hindering the ability to detect new activities effectively. For *DOO-RE*, which has a minimal number of activity classes, a marginal performance dip is seen at batch sizes of 64 or less. This happens because the negatives are fewer than the positives, complicating the task of forming more generalized representations of the known activity amidst irrelevant variations in time series sensor data. Therefore, selecting an optimal batch size requires careful consideration of the number of activity classes and the size of the data in each dataset.

5.6 Visualization

We conduct two types of qualitative analyses: firstly, we use attention maps to assess the quality of invariant representations in each dataset; secondly, we employ T-SNE visualization and scatter plots to evaluate the effectiveness of CLAN and baseline methods in terms of their separation capabilities.

5.6.1 Representations for Each Dataset. In Figure 9, we illustrate how CLAN’s Transformer encoder’s attention maps visually represent the data from all datasets, providing a qualitative assessment of CLAN’s ability to construct representations. The figure is organized into three sections: the first displays the invariant representations learned from known activities, the second shows the representations for test data from known activities, and the third depicts representations for test data from new activities. As our encoder utilizes two layers, we showcase the representations from each layer. The figure shows that the more similar the patterns shown between attention maps, the more likely they are to be the same activity. Several findings are made from this visualization: 1) Across all datasets, the patterns of attention maps in training and test data for a known activity show remarkable similarities. This implies that CLAN is proficient in learning invariant representations. 2) When a new activity is introduced in the test data, the resulting representation diverges significantly from the trained representation of the known activity. This divergence indicates CLAN’s ability to detect representational novelty as a new activity. 3) The visualization also allows us to understand the core features of each activity. For instance, the early and late

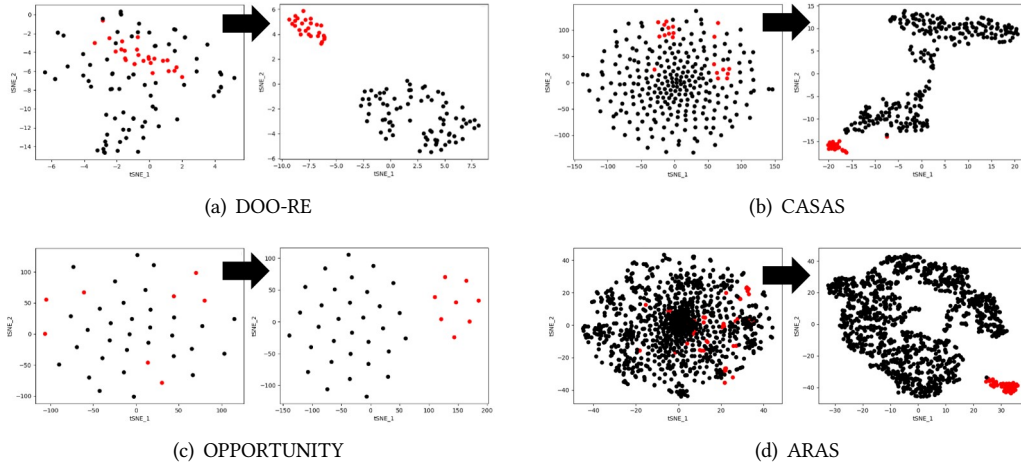


Fig. 10. T-SNE visualization [23] of latent spaces before and after applying CLAN for all datasets. The red dots are samples from a known activity, and the black dots indicate samples from the new activity.

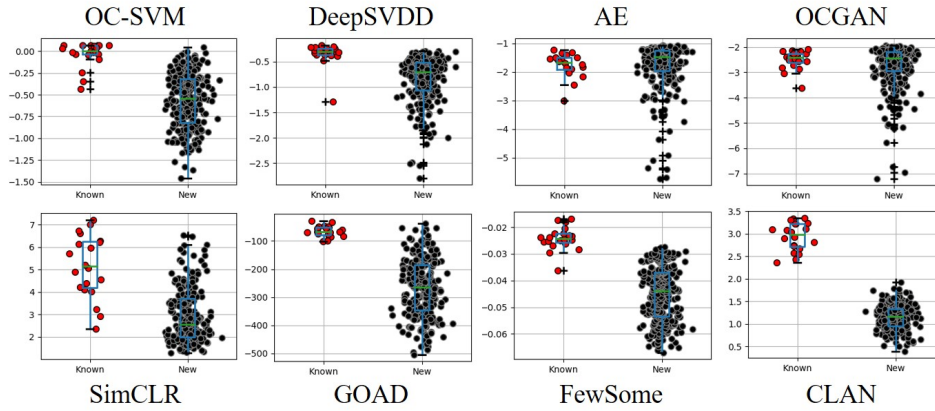


Fig. 11. Scatter plot visualization of each method’s novelty detection score distribution in CASAS. The red dots are samples from the known activity, and the black dots indicate samples from the new activity.

stage patterns in the attention maps are crucial in the known class *Small talk* within *DOO-RE* dataset, whereas the patterns occurring in the early to mid-late stages are significant in known class *Filling the medication dispenser* in *CASAS*. This method of visualization offers insights into interpreting both known and new activities in practical scenarios, as further elaborated in Appendix K.

5.6.2 Separation Ability. Figure 10 demonstrates how CLAN successfully differentiates between known and novel activities through T-SNE visualization [23] for all datasets. The images of the latent space on the right side of each pair demonstrate that known activity samples form distinct clusters, which are clearly separated from the new activity samples. This separation highlights CLAN’s qualitative edge in learning representations, enhancing

its ability to differentiate between known and new activities. This effectively demonstrates CLAN’s superior ability in representation separation across all datasets, further underscoring its generalizability.

To qualitatively assess the distinctiveness of representations with various novelty detection methods, we employ scatter plots supplemented by box plots, as illustrated in Figure 11. The discrepancy in training techniques and scoring mechanisms across baselines renders the novelty detection scores a subjective indicator of their discriminative capacity. It is noticeable that CLAN’s scores for new activities, depicted as black dots, cluster tightly, distinctly separated from the scores for known activities, shown as red dots. We find that CLAN has a clearly larger gap between the scores of known activity and the new activity, compared to other baselines. Additionally, we present box plots superimposed on the scatter plot, where the minimal overlap between the boxes of CLAN’s known and new activities visually underscores the method’s efficacy. This qualitatively shows that CLAN does not only learn representation by focusing on novelty detection but also maintains a balanced expressiveness power of known activities. These findings echo the performance pattern of the CASAS benchmark, as detailed in Table 2.

6 CONCLUSION

This study introduces CLAN, a novel framework for detecting new activities in HAR. CLAN is a Two Tower Contrastive Learning with a Diverse Data Augmentation-based Novelty Detection Framework, which leverages self-supervised learning techniques to construct invariant representations by comparing various types of negatives in both the time and frequency domains. Furthermore, CLAN includes a classification-based selector to automatically determine data augmentation methods based on known activity types within each dataset. Extensive experiments conducted on real human activity datasets demonstrate that CLAN outperforms current state-of-the-art novelty detection approaches in unsupervised settings. The ablation studies highlight CLAN’s data augmentation method selection strategy and the effectiveness of each component of CLAN, showing that CLAN leads to more effective invariant representations that can distinguish between known and new activities. We also present discussions of the key parameters for CLAN operation, various visualizations for qualitative evaluation, and applicability in the real world, providing an overall insight into the robustness of CLAN. The future work and discussion points are described in Appendix M.

In conclusion, CLAN presents a robust and innovative approach to detecting new activities in HAR, offering improved performance and insights into the data augmentation process in time series sensor data. We contend that our work serves as a valuable reference for future sensor-based time series research endeavors, as it sheds light on promising avenues for both representation learning and novelty detection.

REFERENCES

- [1] 2022. *U.S. Bureau of Labor Statistics*. <https://www.bls.gov/tus/> Accessed on September 15, 2023.
- [2] Pimentel Marco AF, David A. Clifton, Lei Clifton, and Lionel Tarassenko. 2014. A review of novelty detection. *Signal processing* 99 (2014), 215–249.
- [3] Jake K. Aggarwal and Michael S. Ryoo. 2011. Human activity analysis: A review. *Acm Computing Surveys (Csur)* 43, 3 (2011), 1–43.
- [4] Haldun Akoglu. 2018. User’s guide to correlation coefficients. *Turkish journal of emergency medicine* 18, 3 (2018), 91–93.
- [5] Hande Alemdar, Halil Ertan, Ozlem Durmaz Incel, and Cem Ersoy. 2013. ARAS human activity datasets in multiple homes with multiple residents. In *7th International Conference on Pervasive Computing Technologies for Healthcare and Workshops*. 232–235.
- [6] Arundo Analytics. 2020. *tsaug: Python package for time series augmentation*. <https://tsaug.readthedocs.io/en/stable/> Accessed on September 15, 2023.
- [7] Dor Bank, Noam Koenigstein, and Raja Giryes. 2023. Autoencoders. *Machine Learning for Data Science Handbook: Data Mining and Knowledge Discovery Handbook* (2023), 353–374.
- [8] Niamh Belton, Misgina Tsighe Hagos, Aonghus Lawlor, and Kathleen M. Curran. 2023. FewSOME: One-Class Few Shot Anomaly Detection With Siamese Networks. In *Proceedings of the IEEE/CVF Conference on Computer Vision and Pattern Recognition*. 2977–2986.
- [9] Asma Benmansour, Abdelhamid Bouchachia, and Mohammed Feham. 2015. Multioccupant activity recognition in pervasive smart home environments. *ACM Computing Surveys (CSUR)* 48, 3 (2015), 1–36.

- [10] Liron Bergman and Yedid Hoshen. 2020. Classification-Based Anomaly Detection for General Data. In *International Conference on Learning Representations*.
- [11] E. Oran Brigham. 1988. *The fast Fourier transform and its applications*. Prentice-Hall, Inc.
- [12] Chengwei Chen, Yuan Xie, Shaohui Lin, Ruizhi Qiao, Jian Zhou, Xin Tan, Yi Zhang, and Lizhuang Ma. 2021. Novelty detection via contrastive learning with negative data augmentation. arXiv:2106.09958 <https://arxiv.org/abs/2106.09958>
- [13] Kaixuan Chen, Dalin Zhang, Lina Yao, Bin Guo, Zhiwen Yu, and Yunhao Liu. 2021. Deep learning for sensor-based human activity recognition: Overview, challenges, and opportunities. *ACM Computing Surveys (CSUR)* 54, 4 (2021), 1–40.
- [14] Ling Chen, Rong Hu, Menghan Wu, and Xin Zhou. 2023. HMGAN: A Hierarchical Multi-Modal Generative Adversarial Network Model for Wearable Human Activity Recognition. In *Proceedings of the ACM on Interactive, Mobile, Wearable and Ubiquitous Technologies*, Vol. 7. 1–27.
- [15] Ting Chen, Simon Kornblith, Mohammad Norouzi, and Geoffrey Hinton. 2020. A simple framework for contrastive learning of visual representations. In *International conference on machine learning*. 1597–1607.
- [16] Dongzhou Cheng, Lei Zhang, Can Bu, Hao Wu, and Aiguo Song. 2023. Learning hierarchical time series data augmentation invariances via contrastive supervision for human activity recognition. *Knowledge-Based Systems* 276 (2023), 110789.
- [17] Heng-Tze Cheng, Feng-Tso Sun, Martin Griss, Paul Davis, Jianguo Li, and Di You. 2013. Nuactiv: Recognizing unseen new activities using semantic attribute-based learning. In *Proceeding of the 11th annual international conference on Mobile systems, applications, and services*. 361–374.
- [18] Grazia Cicirelli, Roberto Marani, Antonio Petitti, Annalisa Milella, and Tiziana D’Orazio. 2021. Ambient assisted living: a review of technologies, methodologies and future perspectives for healthy aging of population. *Sensors* 21, 10 (2021), 3549.
- [19] Israel Cohen, Yiteng Huang, Jingdong Chen, and Jacob Benesty. 2009. Pearson correlation coefficient. *Noise reduction in speech processing* (2009), 1–4.
- [20] Andrew A. Cook, Göksel Mısırlı, and Zhong Fan. 2019. Anomaly detection for IoT time-series data: A survey. *IEEE Internet of Things Journal* 7, 7 (2019), 6481–6494.
- [21] L. Minh Dang, Kyungbok Min, Hanxiang Wang, Md Jalil Piran, Cheol Hee Lee, and Hyeonjoon Moon. 2020. Sensor-based and vision-based human activity recognition: A comprehensive survey. *Pattern Recognition* 108 (2020), 107561.
- [22] Shohreh Deldari, Hao Xue, Aaqib Saeed, Daniel V. Smith, and Flora D. Salim. 2022. Cocoa: Cross modality contrastive learning for sensor data. In *Proceedings of the ACM on Interactive, Mobile, Wearable and Ubiquitous Technologies*, Vol. 6. 1–28.
- [23] Van der Maaten Laurens and Geoffrey Hinton. 2008. Visualizing data using t-SNE. *Journal of machine learning research* 9, 11 (2008).
- [24] Emadeldeen Eldele, Mohamed Ragab, Zhenghua Chen, Min Wu, Chee Keong Kwoh, Xiaoli Li, and Cuntai Guan. 2021. Time-series representation learning via temporal and contextual contrasting. arXiv:2106.14112 <https://arxiv.org/abs/2106.14112>
- [25] Eleazar Eskin. 2000. Anomaly Detection over Noisy Data Using Learned Probability Distributions. In *Proceedings of the Seventeenth International Conference on Machine Learning*. 255–262.
- [26] Ehab Essa and Islam R. Abdelmaksoud. 2023. Temporal-channel convolution with self-attention network for human activity recognition using wearable sensors. *Knowledge-Based Systems* 278 (2023), 110867.
- [27] Kim Eunju, Sumi Helal, and Diane Cook. 2009. Human activity recognition and pattern discovery. *IEEE pervasive computing* 9, 1 (2009), 48–53.
- [28] Donelson R Forsyth. 2018. *Group dynamics*. Cengage Learning, USA.
- [29] Yunhao Ge, Yao Xiao, Zhi Xu, Xingrui Wang, and Laurent Itti. 2022. Contributions of shape, texture, and color in visual recognition. In *European Conference on Computer Vision*. 369–386.
- [30] Tirthankar Ghosal, Tanik Saikh, Tameesh Biswas, Asif Ekbal, and Pushpak Bhattacharyya. 2022. Novelty detection: A perspective from natural language processing. *Computational Linguistics* 48, 1 (2022), 77–117.
- [31] Ian Goodfellow, Jean Pouget-Abadie, Mehdi Mirza, Bing Xu, David Warde-Farley, Sherjil Ozair, Aaron Courville, and Yoshua Bengio. 2020. Generative adversarial networks. *Commun. ACM* 63, 11 (2020), 139–144.
- [32] Robert M. Gray and David L. Neuhoff. 1998. Quantization. *IEEE transactions on information theory* 44, 6 (1998), 2325–2383.
- [33] Trevor Hastie, Robert Tibshirani, Jerome H. Friedman, and Jerome H. Friedman. 2009. *The elements of statistical learning: data mining, inference, and prediction*. Vol. 2. New York: Springer.
- [34] He, Kaiming and Xiangyu Zhang and Shaoqing Ren and Jian Sun 2016. *Deep residual learning for image recognition*.
- [35] Christopher E. Heil and David F. Walnut. 1989. Continuous and discrete wavelet transforms. *SIAM review* 31, 4 (1989), 628–666.
- [36] Dan Hendrycks, Mantas Mazeika, Saurav Kadavath, and Dawn Song. 2019. Using self-supervised learning can improve model robustness and uncertainty. In *Advances in neural information processing systems*, Vol. 32.
- [37] HM Sajjad Hossain, Md Abdullah Al Hafiz Khan, and Nirmalya Roy. 2017. Active learning enabled activity recognition. *Pervasive and Mobile Computing* 38 (2017), 312–330.
- [38] Yash Jain, Chi Ian Tang, Chulhong Min, Fahim Kawsar, and Akhil Mathur. 2022. Collossl: Collaborative self-supervised learning for human activity recognition. In *Proceedings of the ACM on Interactive, Mobile, Wearable and Ubiquitous Technologies*, Vol. 6. 1–28.

- [39] Ashish Jaiswal, Ashwin Ramesh Babu, Mohammad Zaki Zadeh, Debapriya Banerjee, and Fillia Makedon. 2020. A survey on contrastive self-supervised learning. *Technologies* 9, 1 (2020), 2.
- [40] John Taylor Jewell, Vahid Reza Khazaie, and Yalda Mohsenzadeh. 2022. One-class learned encoder-decoder network with adversarial context masking for novelty detection. In *Proceedings of the IEEE/CVF winter conference on applications of computer vision*. 3591–3601.
- [41] Charmi Jobanputra, Jatna Bavishi, and Nishant Doshi. 2019. Human activity recognition: A survey. *Procedia Computer Science* 155 (2019), 698–703.
- [42] Ruimin Ke, Yifan Zhuang, Ziyuan Pu, and Yinhai Wang. 2020. A smart, efficient, and reliable parking surveillance system with edge artificial intelligence on IoT devices. *IEEE Transactions on Intelligent Transportation Systems* 22, 8 (2020), 4962–4974.
- [43] Hyunju Kim and Dongman Lee. 2021. Adela: attention based deep ensemble learning for activity recognition in smart collaborative environments. In *Proceedings of the 36th Annual ACM Symposium on Applied Computing*. 436–444.
- [44] Hyunju Kim and Dongman Lee. 2021. AR-T: Temporal Relation Embedded Transformer for the Real World Activity Recognition. In *In International Conference on Mobile and Ubiquitous Systems: Computing, Networking, and Services*. 617–633.
- [45] Farzana Kulsoom, Sanam Narejo, Zahid Mehmood, Hassan Nazeer Chaudhry, Ayesha Butt, and Ali Kashif Bashir. 2022. A review of machine learning-based human activity recognition for diverse applications. *Neural Computing and Applications* 34, 21 (2022), 18289–18324.
- [46] Hao Lang, Yinhe Zheng, Yixuan Li, Jian Sun, Fei Huang, and Yongbin Li. 2023. *A Survey on Out-of-Distribution Detection in NLP*. arXiv:2305.03236 <https://arxiv.org/abs/2305.03236>
- [47] Bing Li, Wei Cui, Wei Wang, Le Zhang, Zhenghua Chen, and Min Wu. 2021. Two-stream convolution augmented transformer for human activity recognition. In *In Proceedings of the AAAI Conference on Artificial Intelligence*, Vol. 35. 286–293.
- [48] Zhihan Li, Youjian Zhao, Jiaqi Han, Ya Su, Rui Jiao, Xidao Wen, and Dan Pei. 2021. Multivariate time series anomaly detection and interpretation using hierarchical inter-metric and temporal embedding. In *Proceedings of the 27th ACM SIGKDD conference on knowledge discovery & data mining*. 3220–3230.
- [49] Haojie Ma, Wenzhong Li, Xiao Zhang, Songcheng Gao, and Sanglu Lu. 2019. AttnSense: Multi-level attention mechanism for multimodal human activity recognition. *Proceedings of the Twenty-Eighth International Joint Conference on Artificial Intelligence*, 3109–3115.
- [50] Henrik Madsen. 2007. *Time series analysis*. CRC Press.
- [51] Daisuke Nakai Kazuya Ohara Maekawa, Takuya and Yasuo Namioka. 2016. Toward practical factory activity recognition: unsupervised understanding of repetitive assembly work in a factory. In *Proceedings of the 2016 ACM International Joint Conference on Pervasive and Ubiquitous Computing*. 1088–1099.
- [52] Rytis Maskeliūnas, Robertas Damaševičius, and Sagiv Segal. 2019. A review of internet of things technologies for ambient assisted living environments. *Future Internet* 11, 12 (2019), 259.
- [53] Atsuyuki Miyai, Qing Yu, Daiki Ikami, Go Irie, and Kiyoharu Aizawa. 2023. Rethinking Rotation in Self-Supervised Contrastive Learning: Adaptive Positive or Negative Data Augmentation. In *Proceedings of the IEEE/CVF Winter Conference on Applications of Computer Vision*. 2809–2818.
- [54] Sebastian Münzner, Philip Schmidt, Attila Reiss, Michael Hanselmann, Rainer Stiefelwagen, and Robert Dürichen. 2017. CNN-based sensor fusion techniques for multimodal human activity recognition. In *Proceedings of the 2017 ACM international symposium on wearable computers*. 158–165.
- [55] Sebastian Münzner, Philip Schmidt, Attila Reiss, Michael Hanselmann, Rainer Stiefelwagen, and Robert Dürichen. 2017. CNN-based sensor fusion techniques for multimodal human activity recognition. In *Proceedings of the 2017 ACM international symposium on wearable computers*. 158–165.
- [56] Henri J. Nussbaumer. 1982. *The fast Fourier transform*. Springer Berlin Heidelberg.
- [57] Guansong Pang, Chunhua Shen, Longbing Cao, and Anton Van Den Hengel. 2021. Deep learning for anomaly detection: A review. *ACM computing surveys (CSUR)* 54, 2 (2021), 1–38.
- [58] Liangying Peng, Ling Chen, Zhenan Ye, and Yi Zhang. 2018. Aroma: A deep multi-task learning based simple and complex human activity recognition method using wearable sensors. *Proceedings of the ACM on Interactive, Mobile, Wearable and Ubiquitous Technologies* 2, 2, 1–16.
- [59] Pramuditha Perera, Ramesh Nallapati, and Bing Xiang. 2019. Ocgan: One-class novelty detection using gans with constrained latent representations. In *Proceedings of the IEEE/CVF conference on computer vision and pattern recognition*. 2898–2906.
- [60] John G Proakis. 2007. *Digital signal processing: principles, algorithms, and applications*. Pearson Education India.
- [61] Sita Rani, Aman Kataria, Sachin Kumar, and Prayag Tiwari. 2023. Federated learning for secure IoMT-applications in smart healthcare systems: A comprehensive review. *Knowledge-Based Systems* (2023), 110658.
- [62] Daniel Roggen, Alberto Calatroni, Mirco Rossi, Thomas Holleczek, Gerhard Tröster, Paul Lukowicz, Gerald Pirkel, David Bannach, Alois Ferscha, Jakob Doppler, Clemens Holzmann, Marc Kurz, Gerald Holl, Ricardo Chavarriaga, Hesam Sagha, Hamidreza Bayati, and José del R. Millán. 2010. Collecting complex activity datasets in highly rich networked sensor environments. In *Seventh International Conference on Networked Sensing Systems*. 233–240.

- [63] Lukas Ruff, Robert Vandermeulen, Nico Goernitz, Lucas Deecke, Shoaib Ahmed Siddiqui, Alexander Binder, Emmanuel Müller, and Marius Kloft. 2018. Deep one-class classification. In *International conference on machine learning*. 4393–4402.
- [64] Mayu Sakurada and Takehisa Yairi. 2014. Anomaly detection using autoencoders with nonlinear dimensionality reduction. In *Proceedings of the MLSDA 2014 2nd workshop on machine learning for sensory data analysis*. 4–11.
- [65] Mohammadreza Salehi, Atrin Arya, Barbod Pajoum, Mohammad Otoofi, Amirreza Shaeiri, Mohammad Hossein Rohban, and Hamid R. Rabiee. 2021. Arae: Adversarially robust training of autoencoders improves novelty detection. *Neural Networks* 144 (2021), 726–736.
- [66] Mohammadreza Salehi, Hossein Mirzaei, Dan Hendrycks, Yixuan Li, Mohammad Hossein Rohban, and Mohammad Sabokrou. 2021. *A unified survey on anomaly, novelty, open-set, and out-of-distribution detection: Solutions and future challenges*. arXiv:2110.14051 <https://arxiv.org/abs/2110.14051>
- [67] Bernhard Schölkopf, Robert C. Williamson, Alex Smola, John Shawe-Taylor, and John Platt. 1999. Support vector method for novelty detection. In *Advances in neural information processing systems*, Vol. 12.
- [68] Anwar Shah, Nouman Azam, Bahar Ali, Muhammad Taimoor Khan, and JingTao Yao. 2021. A three-way clustering approach for novelty detection. *Information Sciences* 569 (2021), 650–668.
- [69] Jeffrey S Simonoff. 2012. *Smoothing methods in statistics*. Springer Science & Business Media.
- [70] Geetika Singla, Diane J. Cook, and Maureen Schmitter-Edgcombe. 2010. Recognizing independent and joint activities among multiple residents in smart environments. *Journal of ambient intelligence and humanized computing* 1 (2010), 57–63.
- [71] Wesllen Sousa Lima, Eduardo Souto, Khalil El-Khatib, Roozbeh Jalali, and Joao Gama. 2019. Human activity recognition using inertial sensors in a smartphone: An overview. *Sensors* 19, 14 (2019), 3213.
- [72] Sungho Suh, Vitor Fortes Rey, and Paul Lukowicz. 2023. TASKED: Transformer-based Adversarial learning for human activity recognition using wearable sensors via Self-Knowledge Distillation. *Knowledge-Based Systems* 260 (2023), 110143.
- [73] Jihoon Tack, Sangwoo Mo, Jongheon Jeong, and Jinwoo Shin. 2020. Csi: Novelty detection via contrastive learning on distributionally shifted instances. In *Advances in neural information processing systems*, Vol. 33. 11839–11852.
- [74] Engkarat Techapanurak, Masanori Suganuma, and Takayuki Okatani. 2020. Hyperparameter-free out-of-distribution detection using cosine similarity. In *Proceedings of the Asian conference on computer vision*.
- [75] Ashish Vaswani, Noam Shazeer, Niki Parmar, Jakob Uszkoreit, Llion Jones, Aidan N. Gomez, Łukasz Kaiser, and Illia Polosukhin. 2017. Attention is all you need. *Advances in neural information processing systems* 30.
- [76] Feng Wang and Huaping Liu. 2021. Understanding the behaviour of contrastive loss. In *Proceedings of the IEEE/CVF conference on computer vision and pattern recognition*. 2495–2504.
- [77] Jindong Wang, Yiqiang Chen, Shuji Hao, Xiaohui Peng, and Lisha Hu. 2019. Deep learning for sensor-based activity recognition: A survey. *Pattern recognition letters* 119 (2019), 3–11.
- [78] Rui Wang, Chongwei Liu, Xudong Mou, Kai Gao, Xiaohui Guo, Pin Liu, Tianyu Wo, and Xudong Liu. 2023. Deep Contrastive One-Class Time Series Anomaly Detection. In *Proceedings of the 2023 SIAM International Conference on Data Mining (SDM)*. 694–702.
- [79] Qingsong Wen, Tian Zhou, Chaoli Zhang, Weiqi Chen, Ziqing Ma, Junchi Yan, and Liang Sun. 2022. *Transformers in time series: A survey*. arXiv:2202.07125 <https://arxiv.org/abs/2202.07125>
- [80] Zhirong Wu, Yuanjun Xiong, Stella X. Yu, and Dahua Lin. 2018. Unsupervised feature learning via non-parametric instance discrimination. In *Proceedings of the IEEE conference on computer vision and pattern recognition*. 3733–3742.
- [81] Salisu Wada Yahaya, Ahmad Lotfi, and Mufti Mahmud. 2019. A consensus novelty detection ensemble approach for anomaly detection in activities of daily living. *Applied Soft Computing* 83 (2019), 105613.
- [82] Jingkang Yang, Kaiyang Zhou, Yixuan Li, and Ziwei Liu. 2021. *Generalized out-of-distribution detection: A survey*. arXiv:2110.11334 <https://arxiv.org/abs/2110.11334>
- [83] Jingkang Yang, Kaiyang Zhou, and Ziwei Liu. 2023. Full-spectrum out-of-distribution detection. (2023), 1–16.
- [84] George Zerveas, Srideepika Jayaraman, Anuradha Bhamidipaty Dhaval Patel, and Carsten Eickhoff. 2021. A transformer-based framework for multivariate time series representation learning. In *Proceedings of the 27th ACM SIGKDD conference on knowledge discovery & data mining*. 2114–2124.
- [85] Chaoli Zhang, Tian Zhou, Qingsong Wen, and Liang Sun. 2022. TFAD: A decomposition time series anomaly detection architecture with time-frequency analysis. In *Proceedings of the 31st ACM International Conference on Information & Knowledge Management*. 2497–2507.
- [86] Xiang Zhang, Ziyuan Zhao, Theodoros Tsiligkaridis, and Marinka Zitnik. 2022. Self-supervised contrastive pre-training for time series via time-frequency consistency. In *Advances in Neural Information Processing Systems*, Vol. 35. 3988–4003.
- [87] Yu Zhao, Rennong Yang, Guillaume Chevalier, Ximeng Xu, and Zhenxing Zhang. 2018. Deep residual bidir-LSTM for human activity recognition using wearable sensors. *Mathematical Problems in Engineering* (2018), 1–13.
- [88] Yan Zhen, Huan Liu, Meiyu Sun, Boran Yang, and Puning Zhang. 2022. Adaptive preference transfer for personalized IoT entity recommendation. *Pattern Recognition Letters* 162 (2022), 40–46.

A DETAILS OF DATASETS

Table 7 outlines the various activities present in each dataset, while Table 8 details the different sensors each dataset contains.

Table 7. A description of the activities in each dataset. The numbers in parentheses refer to the numbers assigned to each activity class.

Datasets	Activity Types
DOO-RE	<i>Small talk(1), Studying together(2), Technical discussion(3), Seminar(4)</i>
CASAS	<i>Fill medication dispenser(1), Hang up clothes in the hallway closet(2), Move the couch and coffee table(3), Sit on the couch and read a magazine(4), Sweep the kitchen floor(5), Play a game of checkers(6), Set out ingredients(7), Set dining room table(8), Read a magazine(9), Simulate paying an electric bill(10), Gather food for a picnic(11), Retrieve dishes from a kitchen cabinet(12), Pack supplies in the picnic basket(13), Pack food in the picnic basket(14)</i>
OPPORTUNITY	<i>Relaxing(1), Coffee time(2), Early morning(3), Clean up(4), Sandwich time(5)</i>
ARAS	<i>Going Out(2), Preparing Breakfast(3), Having Breakfast(4), Preparing Lunch(5), Having Lunch(6), Preparing Dinner(7), Having Dinner(8), Washing Dishes(9), Having Snack(10), Sleeping(11), Watching TV(12), Studying(13), Having Shower(14), Toileting(15), Napping(16), Other(1)</i>

Table 8. A description of the sensors in each dataset.

Datasets	Sensor Types
DOO-RE	<i>Seat occupation, Sound level, Brightness level, Light status, Existence status, Projector status, Presenter detection status</i>
CASAS	<i>Motion (M01...M51), Item (I01..I08), Cabinet (D01..D12)</i>
OPPORTUNITY	<i>242 sensors including Spoon accelerometer (accX, gyroX, gyroY), Sugar jar accelerometer (accX, gyroX, gyroY), Dishwater reed switch, Fridge reed switch, Left shoe inertial measurement, User location, etc. For more detailed sensor information, see https://archive.ics.uci.edu/ml/datasets/opportunity+activity+recognition.</i>
ARAS	<i>Wardrobe photocell, Convertible couch photocell, TV receiver IR, Couch force , Couch force_2, Chair distance, Chair distance_2, Fridge photocell, Kitchen drawer photocell, Wardrobe photocell, Bathroom cabinet photocell, House door contact , Bathroom door contact, Shower cabinet door contact , Hall sonar distance, Kitchen sonar distance, Tap distance, Water closet distance, Kitchen temperature, Bed force</i>

B BASELINES

We compare CLAN with seven representative novelty detection baselines based on unsupervised learning.

OC-SVM⁵ [67] employs kernel functions to find a hyperplane that best encapsulates the majority of known class samples, effectively identifying a new class sample as those lying outside this hyperplane.

DeepSVDD⁶ [63] learns a hypersphere in the feature space that encapsulates features of known class samples while aiming to minimize the volume of that hypersphere, allowing it to identify a new class sample as those lying outside the learned hypersphere boundary.

AE⁷ [59, 64] utilizes autoencoders (AE) to leverage the reconstruction of known class samples, while they identify a new class sample by detecting when the reconstruction error exceeds a predefined threshold.

OC-GAN⁸ [59] amalgamates the ability of generative adversarial networks (GANs) into one-class classification, generating synthetic data that closely mimics predefined a known class and identifies a new class sample through reconstruction errors.

SimCLR⁹ [8, 73] trains a neural network to obtain representations of a known class by maximizing the similarity of a sample with various augmented samples, and then utilizes the similarity score for novelty detection.

GOAD¹⁰ [10] initially transforms the known data samples into multiple subspaces and optimizes a feature space where inter-class distances are greater than intra-class distances. They use this feature space to gauge novelty likelihood based on the distance from cluster centers and extend its applicability to non-image data through the incorporation of affine transformations.

FewSOME¹¹ [8] employs a Siamese-like architecture with shared-weight neural network branches to transform data samples into closely proximate representations and utilizes a proposed loss called *Stop Loss* to mitigate Representational Collapse. Novelty is detected by the calculated distance between the representations of the new class and the known class samples.

⁵<https://github.com/hiram64/ocsvm-anomaly-detection>

⁶<https://github.com/lukasruff/Deep-SVDD-PyTorch>

⁷<https://github.com/PramuPerera/OCGAN>

⁸<https://github.com/PramuPerera/OCGAN>

⁹<https://github.com/alinalab/CSI>

¹⁰<https://github.com/lironber/GOAD>

¹¹<https://github.com/niamhbelton/FewSOME>

C DESCRIPTION OF APPLIED DATA AUGMENTATION METHODS

Table 9 describes 10 types of data augmentation methods for sensor-based time series used in this paper. Words enclosed within *italics* signify parameters that can be employed with each data augmentation method. Values enclosed in parentheses denote specific experimental values used during the experiments and they are drawn from commonly utilized configurations in previous studies or library [6, 16, 24, 86].

Table 9. Description of 10 types of data augmentation methods for sensor-based time series used in this paper.

Types	Description and implementation details
AddNoise	Injects random Gaussian noise into the input time series data, with the noise's intensity scaled by a factor of <i>scale_num</i> (0.01).
Convolve	Performs a convolution operation on the input time series data using a specified <i>kernel window type</i> (flattop) and a <i>window_size</i> (11).
Permute	Segments the time series data into a variable number of sections between <i>min_segments</i> (1) and <i>max_segments</i> (5) and then reshuffles these segments.
Drift	Gradually shifts the values of the time series data, with the maximum shift magnitude controlled by <i>max_drift</i> (0.7), and the number of affected data points determined by <i>n_drift_points</i> (5).
Dropout	Randomly omits data points in the time series with a probability of <i>p</i> (10%) and replaces them with a specified fill value (0).
Pool	Aggregates time series data within non-overlapping windows of <i>size</i> (4) through a pooling operation, thereby downsampling the time series by selecting representative values from each window.
Quantize	Discretizes individual data points within the time series into one of a defined number of discrete <i>n_levels</i> (20).
Scale	Adjusts each data point's value by applying random scaling factors drawn from a normal distribution centered around <i>loc</i> (2) with a standard deviation of <i>sigma</i> (1.1).
Reverse	Inverts the temporal order of data points, effectively flipping the sequence of the time series data.
TimeWarp	Modifies the time series data's tempo by introducing up to <i>n_speed_change</i> (5) alterations, where the time axis can be stretched or compressed up to a specified <i>max_speed_ratio</i> (3).

D IMPLEMENTATION DETAILS

We perform experiments on a server that has NVIDIA TITAN RTX GPU, Intel Xeon Gold 5215 CPU (2.5GHz), 256GB RAM, and Ubuntu 18.04.5 LTS OS. The implementation of CLAN is founded on Anaconda 4.10.1, Python 3.7.16, and Pytorch 1.12.1. As a means of ensuring the reproducibility of CLAN, all of the source code and experimental details are publicly accessible on the project’s GitHub repository ¹².

We utilize 10 widely used data augmentation methods in time series [6, 16, 24, 86] including *AddNoise*, *Convolve*, *Permute*, *Drift*, *Dropout*, *Pool*, *Quantize*, *Scale*, *Reverse* and *TimeWarp*, and their details are described in Appendix C. The data augmentation method selector selects the θ_{ST} value from the AUROC value threshold set {0.5, 0.6, 0.7, 0.8, 0.9}. Depending on the type of activity known within each dataset, θ_{ST} is set to the maximum value from which two or more data augmentation methods can be derived. We implement the frequency domain of each sample using Pytorch’s FFT library ¹³. As shown in Section 4.3.5, the Transformer encoder [75] is employed as the backbone and connects the projection network and linear layer on top. The backbone consists of a stack of two encoder layers, where each layer has one attention head and a feedforward neural network with a dimension that is twice the length of the input data. The projection layer is composed of two fully connected (linear) layers along with batch normalization and a ReLU activation function, to convert the extracted backbone features into 128-dimensional embedding feature vectors [86]. The linear layer is a single layer that scales the feature output in dimensions K to match the number of data augmentation method types. We train the encoders using the Adam optimizer with $3e^{-4}$ learning rate and configure the loss function with $\tau = 0.5$.

As the baselines are designed for image data, the input format is converted from images to sensor-based time series data, and the neural network or training method is adapted to accommodate this change. To ensure a fair and consistent comparison, the identical training strategy is implemented throughout all experiments in both the baselines and CLAN. Z-score normalization [55] is applied to all datasets, and a mini-batch method with a batch size of 64 is used, spanning 100 training epochs. Better results are selected between the original architecture and the Transformer encoder for baselines. We perform experiments using 10 different random seeds and report the average performance. The dataset is divided into training and test subsets in the 80:20 ratio. The training dataset consists of samples of known activity, while the test dataset contains both known and new activity samples.

¹²The code will be available after the paper is published.

¹³<https://pytorch.org/docs/stable/fft.html>

E CLASSIFICATION RESULTS BETWEEN ORIGINAL DATA AND SHIFTED DATA

We derive classification results between original data and shifted data for all data as shown in Figure 12, 13, 14. Each result is denoted as $\alpha_{\mathcal{T}}$. As described in Table 1 and the figures, the classification performance for *AddNoise* is consistently low across all datasets, and this augmentation method is not classified as *ST* across all datasets. This data augmentation is commonly used to create positives. Conversely, *Reverse* consistently shows high classification performance across all datasets, leading it to be classified as *ST* in all of them. When inspecting *Convolve*, the classification performance is low on the *DOO-RE* dataset, but high on the other datasets. *Convolve* is classified as *ST* only in datasets other than *DOO-RE* dataset. In addition, the degree of data shift varies by time or frequency domain. The *Scale* method demonstrates approximately 70% classification performance in the time domain, but it exhibits higher performance in the sensor frequency domain. Therefore, *Scale* may not belong to *ST* in the temporal aspect, but in the frequency aspect, it is considered one of the *ST* of all datasets. In this way, CLAN incorporates both an ST^T that helps to generate negatives in the time domain and an ST^F that generates negatives in the frequency domain for each activity.

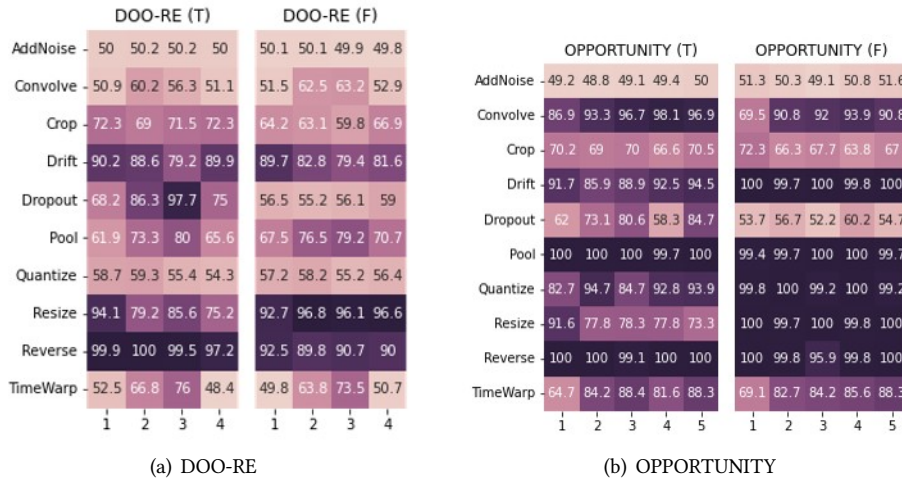
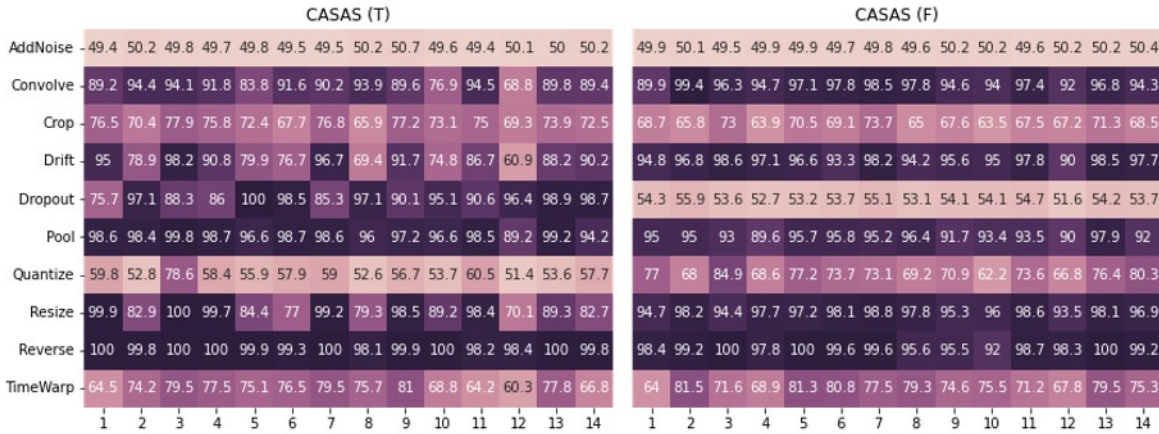
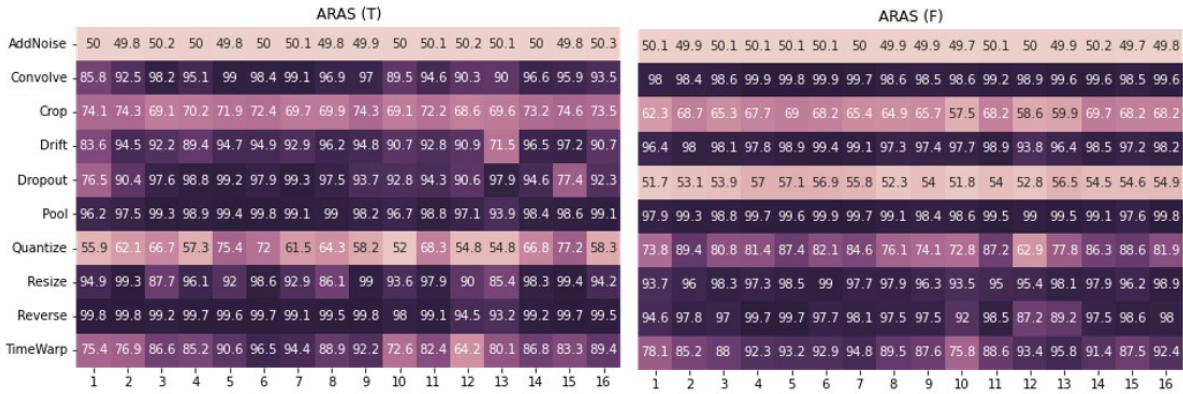


Fig. 12. Classification results between original and shifted data in *DOO-RE* and *OPPORTUNITY*.



(a) CASAS

Fig. 13. Classification results between original and shifted data in CASAS.



(a) ARAS

Fig. 14. Classification results between original and shifted data in ARAS.

F EFFECT OF SELECTING APPROPRIATE *ST* FOR EACH DATASET

We conduct a simple experiment on why we need to apply a different *ST* for each dataset and for each dataset-specific activity class. *Customized* in the table indicates customizes *ST* for each activity of each dataset as do in CLAN, while the *Same* environment applies the same augmentation methods (DOO-RE’s first activity classes in *ST* of DOO-RE) to all datasets. As shown in Table 10, the detection performance drops 0.8%, 9.1%, 0.8%, and 22.5% of DOO-RE, CASAS, OPPORTUNITY, and ARAS datasets, respectively. As shown in the DOO-RE dataset’s performance degradation, applying the same *ST* within the same dataset also raises performance degradation to other activity classes’ performance. This is a phenomenon that occurs because each time series dataset has different captured behaviors and sensor modalities, and proves that a customized data augmentation strategy is needed to reflect the characteristics of each dataset and behavior class to create invariant representations.

Table 10. AUROC (%) performance comparison between applying the customized *ST* of CLAN and applying the same *ST* to all activity classes in all datasets (here, applying *ST* in the first activity class of DOO-RE).

Dataset	DOO-RE	CASAS	OPPORTUNITY	ARAS
Customized	95.8 (± 3.2)	98.7 (± 1.5)	98.0 (± 2.0)	94.9 (± 4.8)
Same	95.0 (± 4.2)	90.5 (± 8.1)	97.2 (± 2.0)	77.5 (± 11.1)

G ROC CURVE GRAPHS OF THE *OPPORTUNITY* AND *ARAS* DATASETS

Figure 15 shows ROC curve graphs of the *OPPORTUNITY* and *ARAS* datasets. This highlights CLAN’s uniformly high performance in all one-class classification tasks, going beyond average performance. It reveals how CLAN effectively distinguishes between activities, avoiding irrelevant temporal dynamics or similar characteristics across different activities even in *OPPORTUNITY* and *ARAS* datasets. CLAN demonstrates a robust ability to maintain performance in multi-class configurations, outperforming other baseline methods. This advantage is due to its approach of accounting for variations in individual samples across both time and frequency domains, which results in the creation of more effective invariant representations for a variety of activities.

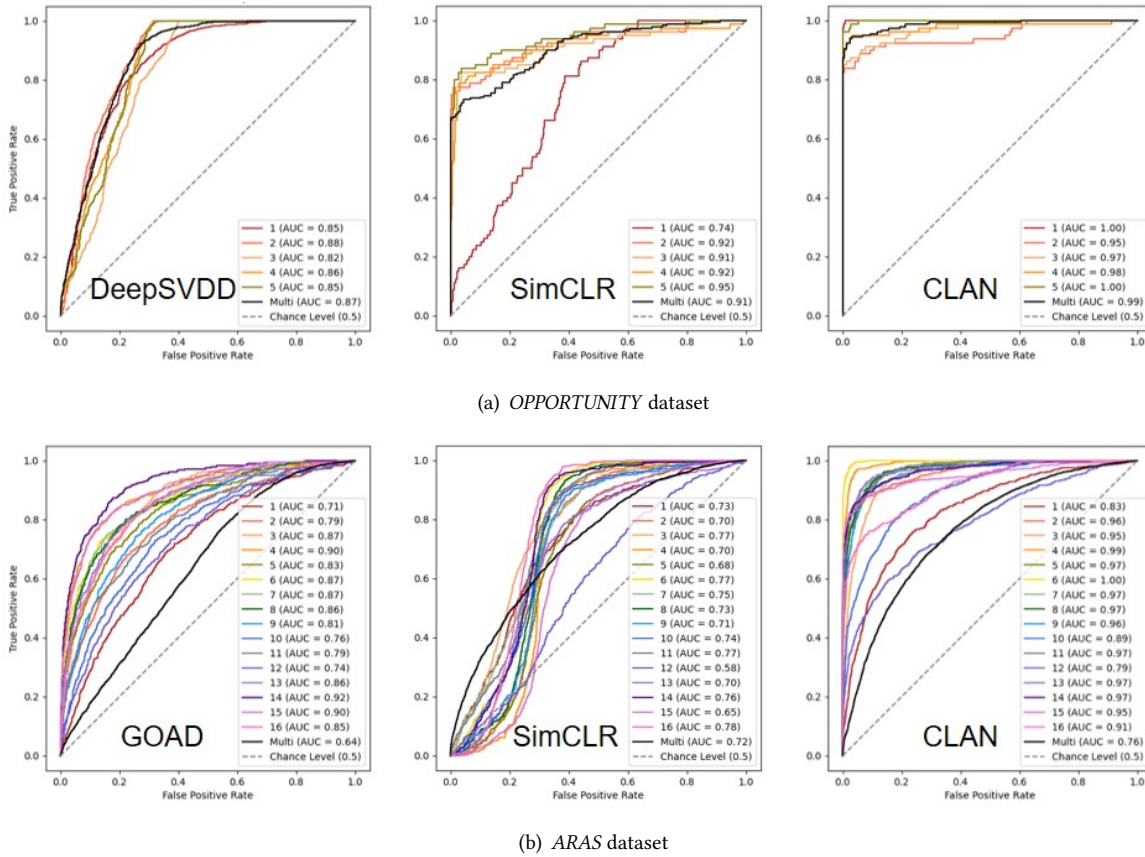


Fig. 15. ROC curve graphs for the *OPPORTUNITY* and *ARAS* datasets. We draw figures of CLAN and two baselines that provide decent performance for each dataset. The positioning of the ROC graph closer to the top-left corner indicates superior performance. The numerical labels on each ROC curve graph correspond to the distinct activities in each dataset, as detailed in Appendix A. The value in parentheses next to each activity indicates the performance of one-class classification for that activity. ROC curves labeled as *Multi* display the mean performance across multi-class scenarios.

H EFFECT OF ST CONFIGURATION

In a finite set of data augmentation techniques, as the parameter θ_{ST} is increased, the range of available augmentation methods becomes narrower, but these methods yield samples with more significant shifts. On the other hand, when the value of θ_{ST} is lower, a greater variety of augmentation techniques are accessible, although they tend to generate samples with smaller shifts and require more computational time. For effectively capturing invariant representations in time series sensor data, which inherently contain various variations, it's crucial to maintain both a high quantity and quality of negative samples.

We conduct a study to understand the impact of varying the amount of data augmentation methods on novelty detection efficiency. Randomly select a data augmentation method listed in Table 9 and test 1 to 9 data augmentation methods to observe their impact on performance. Figure 16(a) and Figure 16(b) demonstrate that performance is enhanced with the usage of a broader range of data augmentation methods, given the same augmentation set is applied. However, it's crucial to note that as we broaden the range of methods, the time taken for inference also increases correspondingly. For both datasets, noticeable changes in novelty detection performance are observed when the number of data augmentation methods increases from one to two.

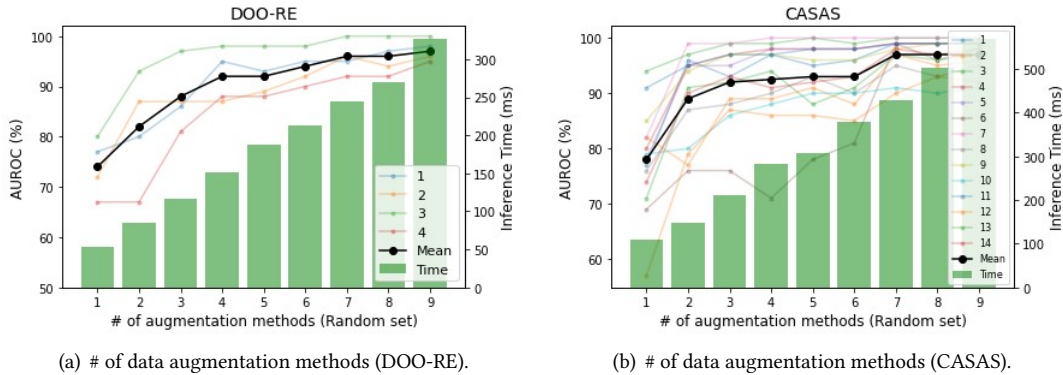


Fig. 16. AUROC (%) performance changes according to the number of data augmentation methods in *DOO-RE* and *CASAS*. The numerical labels on each graph correspond to the distinct activities in each dataset, as detailed in Appendix A.

Figures 17(a) and 17(b) illustrate how performance varies with respect to $\alpha_{\mathcal{T}}$, under conditions of equal data augmentation method count. It is observed that utilizing data augmentation methods more closely aligned with $\alpha_{\mathcal{T}}$ for creating negative samples leads to improved novelty detection effectiveness. This result is consistent with the results of Table 4.

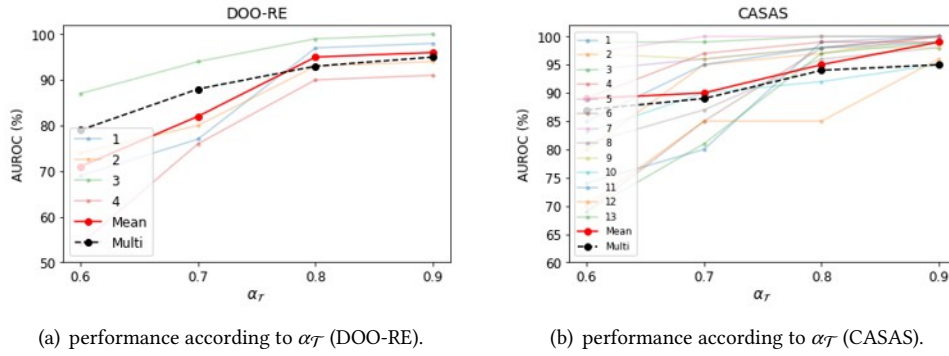


Fig. 17. AUROC (%) performance changes according to $\alpha_{\mathcal{T}}$. The numerical labels on each graph correspond to the distinct activities in each dataset, as detailed in Appendix A.

I EFFECTS OF BALANCING TERM λ

We test whether the balancing terms inspired by the previous paper [73] still work on time series sensor data for HAR, as shown in Table 11. The parameters are applied in Equation (13) and (14) in CLAN. While this parameter shows limited enhancement in one-class configurations, it proves to be substantially beneficial in boosting the performance in multi-class setups.

Table 11. Effects of balanced terms λ .

	DOO-RE		CASAS		OPPORTUNITY		ARAS	
	w	w/o	w	w/o	w	w/o	w	w/o
One-class setup	95.8	96.0	98.7	98.2	98.0	98.3	94.9	92.4
Multi-class setup	96.3	95.7	95.7	90.3	98.8	98.4	77.9	74.2

J EFFECTS OF LEARNING RATE

The learning rate plays a crucial role in representation learning. A higher learning rate might accelerate the training process but risks surpassing the best solution, causing instability or divergence. Conversely, a lower learning rate offers steadier and more accurate progress towards the optimal point, but this can greatly decelerate training and potentially lead to becoming trapped in local minima. In our experiments across all datasets, we test learning rates from $1e-1$ to $1e-6$ as shown in Figure 18. The results indicate that when dealing with time series sensor data in CLAN, a learning rate between $1e-3$ to $1e-4$ yields the best outcomes. This finding can guide the selection of a fixed learning rate or the adjustment of a learning rate scheduler.

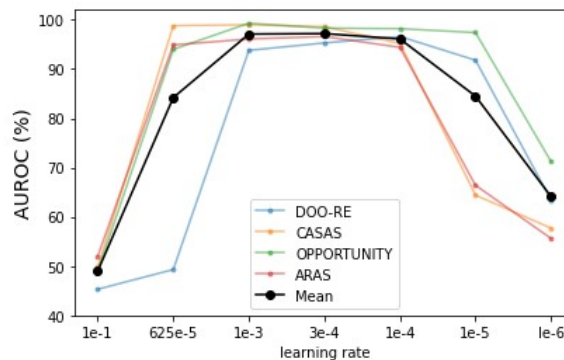


Fig. 18. Effects of learning rates from $1e-1$ to $1e-6$ for all datasets.

K EXPLAINABILITY OF CLAN

Figure 19 illustrates the use of attention maps (i.e. extracted representations) from CLAN. Each line's attention map pair shows the representations from the perspectives of time and sensor. The first line's attention maps reveal the invariant representations learned from a known activity (Filling the medication dispenser - occurs within the area marked by the red box). Utilizing the invariant representations from the known activity, the representations of test data from the known activity are shown in the second line, and the representations of test data from a new activity (Hang up clothes in the hallway closet - happens within the area marked by the blue box) are displayed in the third line.

When comparing the three attention map lines, it becomes evident that the representations of the known activity test data (second line) bear greater resemblance to the learned representation (first line) than the representations of the new activity test data (third line). When a new activity is detected in this way, new representations such as the fourth one can be learned about this activity to obtain representations suitable for this activity. When a new activity is detected in this manner, CLAN's learning process enables the extraction of new representations (fourth line), serving as invariant representations for this activity. Additionally, the characteristics of the known activity become clear through the acquired representations. Regarding Activity 1, it can be interpreted that the correlations between the start and finish of user action patterns are crucial, especially when the motion sensors in the red boxes are activated.

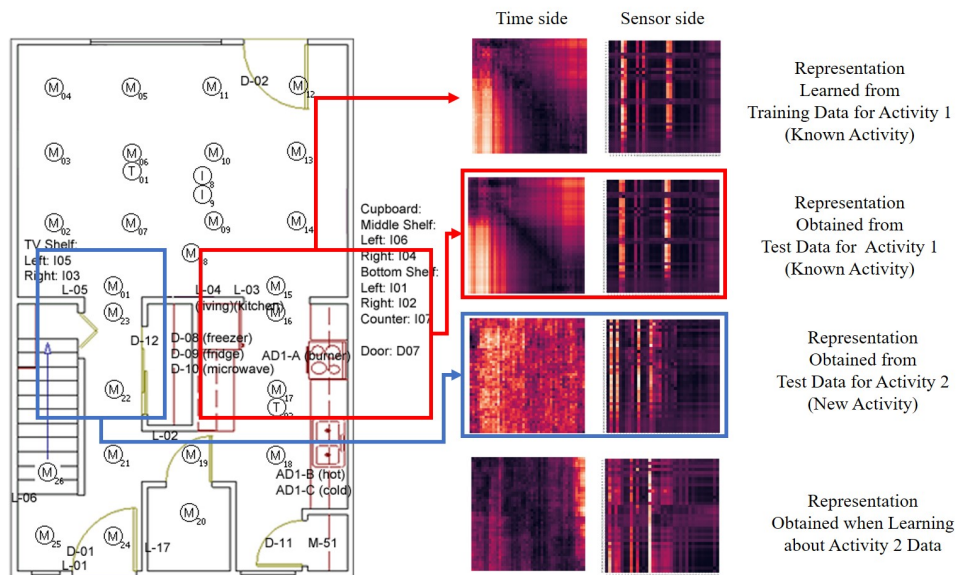


Fig. 19. Explainability of CLAN. The characteristics of activities can be understood using the representations drawn with the attention maps extracted from CLAN. The room structure picture is referred from CASAS [70].

L APPLICABILITY

L.1 Performance Robustness to Training Data Size

The experiment is performed to evaluate the impact of varying data sizes on CLAN’s performance, as shown in Figure 20. It begins by utilizing the entire training data set and then progressively decreases the data size to 20% of its initial size, in steps of 20% reductions. The mean peak performance of the baselines is depicted by a black dotted line. Notably, CLAN exceeds these baselines using only 40% of the training data. When trained with merely 20% of the data, CLAN demonstrates impressive results, achieving 90.9% on *DOO-RE*, 89.6% on *CASAS*, 87.7% on *OPPORTUNITY*, and 73.8% on *ARAS*. Comparing the baselines’ performance in Table 2, CLAN outstrips many of the baselines even with 20% of the training data. The results verify CLAN’s practicality in real-world scenarios, showcasing its ability to accurately detect novelties with limited known activity data.

L.2 Inference Time

We conduct a comparative analysis to evaluate the inference times of CLAN in comparison to *FewSome*, known for its effectiveness and efficiency among baseline approaches. We define *inference time* as the average computational duration (*ms*) required to derive features and obtain a novelty score for a single sample. To accurately measure computation time on both GPU and CPU, we use the `cuda synchronize`¹⁴. Summarized in Table 12, CLAN exhibits a remarkable speed advantage, performing 1.2X to 4.2X faster than the baseline method. For all datasets, CLAN shows superiority not only in terms of accuracy but also in terms of time taken for inference. This significant leap in efficiency is due to CLAN’s novelty determination mechanism, achieved through simplified computation of similarity and classification scores. These results provide strong support for the practicality of integrating CLAN into real-time scenarios.

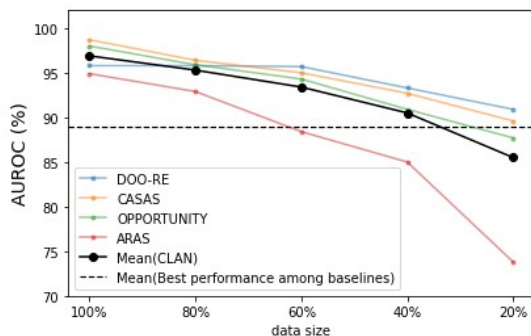


Fig. 20. Performance according to training data size.

Framework	DOO-RE	CASAS	OPP	ARAS
FewSome	31.553	34.760	37.172	32.920
CLAN	7.521	11.360	32.270	8.191

Table 12. Novelty detection inference time (*ms*) for all datasets.

¹⁴<https://pytorch.org/docs/stable/generated/torch.cuda.synchronize.html>

M DISCUSSION AND FUTURE WORK

Through experiments with real-world datasets, we plan to further improve CLAN in four parts.

- (1) Here we experiment with CLAN based on 10 data augmentation methods used on time series sensor data, but combining data augmentation methods, changing the parameters of each data augmentation method, or combining CLAN with more advanced data generation methods such as GAN [14] can produce more sophisticated samples suitable for negatives. This means that CLAN can scale more effectively to more types of datasets, and we expect that this flexibility allow CLAN to spread to a wide range of applications.
- (2) Table 3 shows that there seems to be room to improve the ARAS performance to some extent in the multi-class setup. This is because the number of overlapping features between known and new activities increases, preventing an appropriate invariant representation from being generated. We plan to address this issue by introducing additional discrimination mechanisms based on multiple known activities.
- (3) We intend to create a sustainable HAR system as stated in [27] by integrating CLAN with active learning [37] and recent advanced activity recognition models [14, 16, 26, 44, 47].
- (4) We construct the framework by dividing it into the time domain and frequency domain for generalization purposes here, but CLAN has expandability that can create a more realistic multi-faceted representation by adding user characteristics and sensor characteristics depending on the specific types of data.

Received 15 November 2023